Science of the Total Environment 952 (2024) 175979

Contents lists available at ScienceDirect

Science of the Total Environment

journal homepage: www.elsevier.com/locate/scitotenv

Shedding light on the cellular mechanisms involved in the combined adverse effects of fine particulate matter and SARS-CoV-2 on human lung cells

Sara Marchetti [a,*], Anita Colombo [a], Melissa Saibene [b], Cinzia Bragato [a], Teresa La Torretta [c], Cristiana Rizzi [d], Maurizio Gualtieri [a], Paride Mantecca [a]

[a] POLARIS Research Centre, Department of Earth and Environmental Sciences, University of Milano-Bicocca, Piazza della Scienza 1, 20126 Milano, Italy
[b] Platform of Microscopy, University of Milano-Bicocca, Piazza della Scienza 2, 20126 Milano, Italy
[c] Laboratory of Atmospheric Pollution, National Agency for New Technologies, Energy and Sustainable Economic Development, ENEA, 40129 Bologna, Italy
[d] Department of Earth and Environmental Sciences, University of Milano - Bicocca, Piazza della Scienza, 1, 20126 Milano, Italy

HIGHLIGHTS

- Fine particulate matter ($PM_{2.5}$) as risk factor for the onset of COVID-19 disease.
- PM-driven increased expression of ACE2 increase the infectability of lung cells.
- Enhanced capability of SARS-CoV-2 internalization in $PM_{2.5}$ primed cells.
- $PM_{2.5}$ as factor increasing the inflammatory responses to SARS-CoV-2 infection.

GRAPHICAL ABSTRACT

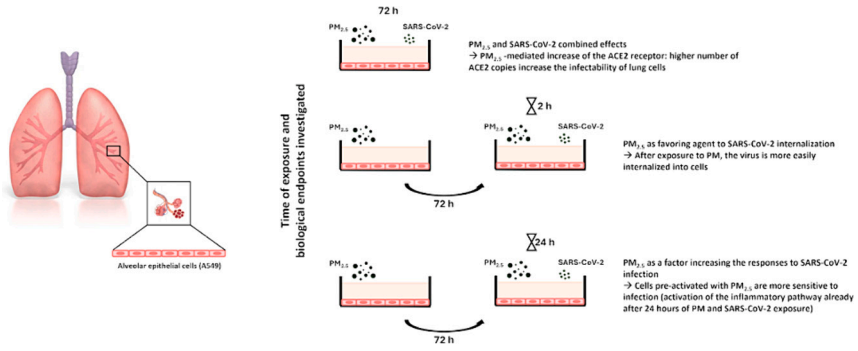

ARTICLE INFO

Editor: Lidia Minguez Alarcon

Keywords:
Particulate matter
Infection
SARS-CoV-2
Inflammation
In vitro study

ABSTRACT

Airborne pathogens represent a topic of scientific relevance, especially considering the recent COVID-19 pandemic. Air pollution, and particulate matter (PM) in particular, has been proposed as a possible risk factor for the onset and spread of pathogen-driven respiratory diseases. Regarding SARS-CoV-2 infection, exposure to fine PM ($PM_{2.5}$, particles with an aerodynamic diameter < 2.5 μm) has been associated with increased incidence of the COVID-19 disease.

To provide useful insights into the mechanisms through which PM might be involved in infection, we exposed human lung cells (A549) to $PM_{2.5}$ and SARS-CoV-2, to evaluate the toxicological properties and the molecular pathways activated when airborne particles are combined with viral particles. Winter $PM_{2.5}$ was collected in a metropolitan urban area and its physico-chemical composition was analyzed. A549 cells were exposed to SARS-CoV-2 concomitantly or after pre-treatment with $PM_{2.5}$. Inflammation, oxidative stress and xenobiotic metabolism were the main pathways investigated. Results showed that after 72 h of exposure $PM_{2.5}$ significantly increased the expression of the angiotensin-converting enzyme 2 (ACE2) receptor, which is one of the keys used

* Corresponding author.
E-mail address: sara.marchetti1@unimib.it (S. Marchetti).

https://doi.org/10.1016/j.scitotenv.2024.175979
Received 15 March 2024; Received in revised form 29 August 2024; Accepted 30 August 2024
Available online 2 September 2024

by the virus to infect host cells. We also analyzed the endosomal route in the process of internalization, by studying the expression of RAB5 and RAB7. The results show that in cells pre-activated with PM and then exposed to SARS-CoV-2, RAB5 expression is significantly increased. The activation of the inflammatory process was then studied. Our findings show an increase of pro-inflammatory markers (NF-kB and IL-8) in cells pre-activated with PM for 72 h and subsequently exposed to the virus for a further 24 h, further demonstrating that the interaction between PM and SARS-CoV-2 determines the severity of the inflammatory responses in lung epithelial cells. In conclusion, the study provides mechanistic biological evidence of PM contribution to the onset and progression of viral respiratory diseases in exposed populations.

1. Introduction

According to the Global Burden of Disease Study (GBD), infectious diseases (IDs) represent a major cause of human morbidity and mortality (Abbafati et al., 2020). Although progress has been made in the treatment and prevention of IDs, the emergence of viral pathogens remains one of the greatest threats to human health (Michaud, 2009).

In recent years, we have faced the COVID-19 pandemic whose pathogen is the Severe Acute Respiratory Syndrome Coronavirus 2 (SARS-CoV-2). The emergence has had, and still is having, a global impact on human health and caused approximately 7 million deaths, as reported by the World Health Organization (WHO) (https://covid19.who.int/). Over the past decades, several infectious diseases caused by viral pathogens have emerged, such as SARS-CoV-1, MERS-CoV, H5N1, H1N1, H7N9 (Wei et al., 2016) and more recently, the aforementioned SARS-CoV-2. It is therefore urgent to understand if, among the possible risk factors underlying the appearance and spread of these diseases, environmental quality may play a role, especially considering that most of these are of zoonotic origin (Michaud, 2009).

Air pollution is considered one of the variables involved in the onset of these diseases, as it is supposed to play a role in the increases in incidence, severity of morbidity and mortality. Numerous studies have already proposed airborne pollutants, and particulate matter (PM) in particular, as important risk factors for respiratory and cardiovascular diseases and therefore they could play a role in conditioning the vulnerability to infections, the development of the pathology and the prognosis of pathogen-driven diseases (Hsiao et al., 2022; Nor et al., 2021; Santurtún et al., 2022). Therefore, surveillance of viral disease outbreaks highlights the need for in-depth investigations on the impact of airborne pollution on respiratory viral infections.

Regarding SARS-CoV-2 infection, it has been suggested that air pollution and more precisely, fine PM ($PM_{2.5}$), CO, and NO_2, may be associated with a greater incidence and severity of clinical manifestations of COVID-19. The hypothesis of a close relationship between virus spread and infectivity and high air pollution has been postulated since the beginning of the pandemic, when a high number of COVID-19 cases was recorded in highly polluted areas (Hernandez Carballo et al., 2022; Loaiza-Ceballos et al., 2022). There is still a lively debate if and whether the SARS-CoV-2 virus can be transmitted via PM. Some authors have suggested that SARS-CoV-2 could be transmitted by indirect contact via the aerosol generated by infected individuals who deposit on PM suspended in environments. Thus, according to this hypothesis, PM should act as a vector for SARS-CoV-2 virions, facilitating its entry in the lung (Nor et al., 2021; Setti et al., 2020). Nevertheless, this hypothesis has not been verified by experimental data. Several studies have focused on the presence of viral genetic material (RNA) in PM filters collected in polluted areas in search of clear evidence. This approach has however led to controversial results (Chirizzi et al., 2021; Licen et al., 2022; Nor et al., 2021; Pivato et al., 2022; Setti et al., 2020). A recent publication provides detailed information on the molecular interactions between PM and SARS-CoV-2 Spike protein. The authors demonstrate that a physical link between PM and SARS-CoV-2 virus is possible, and this link is strong enough to reduce the possibility of infection of the virus (Romeo et al., 2023).

In parallel, some authors have proposed that PM could have a direct and/or indirect systemic impact on the human body thus, reducing resistance to infection and making people more susceptible to pathogens (Bontempi et al., 2020; Conticini et al., 2020; Domingo et al., 2020; Murgia et al., 2021).

In the last decades, numerous studies have investigated the effects of PM in in vitro and in vivo models, depending on its chemical composition and/or size, both in short and long-term exposure. In these studies, exposure to PM has been found to affect lung defense mechanisms and cause chronic inflammation, oxidative stress and genotoxic and mutagenic effects, making the respiratory system more susceptible to viral infections and exacerbating the pathogenesis of respiratory diseases (Botto et al., 2023; Domingo et al., 2020; Loaiza-Ceballos et al., 2022; Longhin et al., 2018; Mantecca et al., 2010; Morakinyo et al., 2016; Sancini et al., 2014; Valavanidis et al., 2008). It is therefore of great relevance to collect data that clarify which interactions PM and SARS-CoV-2 may have on human cells, considering the lung epithelium as the primary target tissue.

The association between SARS-CoV-2 infection and exposure to PM could be explained by the overexpression of the angiotensin-converting enzyme 2 (ACE2) in the human airways, promoted by the pollutant. ACE2 activation is known to occur in response to PM-induced inflammation and oxidative stress as a protective mechanism to reduce the severity of lung damage by inhibiting both the inflammatory response and oxidative stress. In fact, ACE2 acts by inhibiting the intracellular nuclear factor-kB (NF-kB) that is a mediator of the pro-inflammatory response and in parallel, activates the nuclear factor NRF2, which in turn is responsible for the anti-inflammatory response (Fang et al., 2019).

The transmembrane spike (S) glycoprotein of SARS-CoV-2 facilitates viral entry by binding the ACE2 receptor and fusing with human cells. Therefore, the expression of this receptor represents a decisive step in infection (Borkotoky et al., 2023; Praharaj et al., 2022). The transmembrane protease serine type 2 (TMPRSS2) has also been suggested as key enzyme for viral spread. It has been proposed that SARS-CoV-2 uses the ACE2 receptor for entry into target cells and TMPRSS2 for S protein priming. The S protein is in fact composed of S1, which includes the receptor-binding domain (RBD) that binds to ACE2, and the S2 subunit that mediates membrane fusion. Priming of the S protein by proteases is necessary for cellular and viral membranes fusion (Hoffmann et al., 2020a; Iwata-Yoshikawa et al., 2022).

The possible relation between PM exposure and ACE2 expression has been suggested by previous papers (Botto et al., 2023; Li et al., 2021). However, to our knowledge, there are few studies investigating the combined exposure of biological models to PM and SARS-CoV-2, although the possible interactions of airborne and viral particles on the same biological model are extremely relevant to understand the toxicology of SARS infection in urban and polluted areas. Moreover, none of these previous studies investigated at molecular level the effects of the combined exposure.

In a recent study we suggested a plausible biological mechanism that might explain how exposure to urban fine PM can lead to an increase in cellular infection to SARS-CoV-2 (Marchetti et al., 2023). The study highlights the key role played by ACE2 receptor in promoting virus entry in the lung and supports the results of ecological studies showing a positive correlation between COVID-19 cases or mortality associated

with poor air quality.

The present study aims at providing mechanistic insights of the toxicological effects of viral particles when combined with airborne $PM_{2.5}$ exposure at cellular level, also considering the particles physico-chemical composition. After the characterization of the $PM_{2.5}$ collected in a metropolitan urban area, human lung A549 cells exposed to SARS-CoV-2 either concomitantly or after preliminary treatment with $PM_{2.5}$. At the end of the incubation period, the biological mechanisms related to oxidative stress, xenobiotic metabolism and inflammation have been investigated.

2. Material and methods

2.1. PM sampling and extraction

$PM_{2.5}$ was collected at Torre Sarca (Milan, Italy, 45°31′ 18.4″ N 9°12′45.3″E) during winter 2021 (December 2020-March 2021). Particles were collected on glass fiber and Teflon filters using a low-volume gravimetric sampler (Hydra dual sampler, FAI Instruments, Rome, Italy). For biological exposures, Teflon filters were pooled and particles were detached by using an ultrasonic bath (Sonica®, SOLTEC, Milan, Italy) to maximize particle recovery. Particles were recovered from filters in ultra-pure water with four cycles of 20 min each, with a water bath kept within 15 °C by ice, collected in sterile tubes and dried into a desiccator (for more details see Marchetti et al., 2019). Finally, the sterile tubes were differentially weighed before and after extraction to determine the mass of the extracted particles and stored at minus 20 °C until use. For exposure experiments, $PM_{2.5}$ aliquots were suspended in sterile water to obtain suspensions at a final concentration of 2 μg/μL. Particles were sonicated for 30 s just prior to cell exposure. For the detection of Polycyclic Aromatic Hydrocarbons, organic particles were extracted from glass fiber filters with hexane in an ultrasonic bath for 30 min. The extraction solvent was then filtered (0.45 μm) and evaporated with N_2.

2.2. Characterization of particle suspensions

The morphology and size of particles were determined by transmission electron microscopy (TEM) analysis. 25 μg/mL of PM suspension and 2.4×10^3 genome copies/mL of SARS-CoV-2 (ATCC® VR1986HK™) were added dropwise onto a Formvar®-coated 200-mesh copper grid. After o/n drying, TEM micrographs were acquired using a transmission electron microscope (JEM 2100 Plus, JEOL, Japan) operating at an acceleration voltage of 200 kV and equipped with an 8-megapixel (Gatan, US) Rio complementary metal-oxide-superconductor (CMOS) camera.

2.3. Chemical analysis

The total carbon and inorganic carbon content of sampled PM was analyzed on 1 cm^2 glass fiber filter punches selecting different filters along all the sampling campaign. A total carbon analyzer for solid samples measurements was used (Shimazu SSM 5000 A). On the same filters, the ionic species (anion and cation) were quantified by liquid chromatography (ThermoFisher Scientific-Dionex ICS 1100, details in Stracquadanio et al., 2019). PAHs were analyzed on parallel filters by gas chromatography/mass spectrometry according to Marchetti et al., 2021. Finally, metal and trace elements were analyzed by XRF (ED-XRF, NEX CG Rigaku, details in Stracquadanio et al., 2019) on Teflon filters collected in parallel to glass fiber filters covering the same sampling period.

2.4. Endotoxin content

Endotoxin content in the extracted $PM_{2.5}$ was quantified by the Limulus Amebocyte Lysate (LAL) test accordingly to the manufacturer's instructions (Pierce Chromogenic Endotoxin Quant Kit, Thermo Scientific). Briefly, PM extracts were diluted with endotoxin-free LAL reagent water to the concentration of 25 μg/mL. Samples were mixed with LAL reagent and incubated at 37 °C for 12 min before a chromogenic substrate was added followed by additional 6 min of incubation. The reaction was then stopped with 25 % acetic acid and the absorbance of the samples was measured at 405 nm by a spectrophotometer (Tecan, Männedorf). The endotoxin content was calculated from a standard curve of *Escherichia coli* (LPS) and the concentration was expressed as endotoxin units per milligram (EU/mg) of tested particles.

2.5. Cell culture and exposure

The A549 cell line, that have been extensively used in studies of infection with intact SARS-CoV-2 viruses (Chu et al., 2020; Hoffmann et al., 2020b; Schreiber et al., 2022), is representative of lung type 2 alveolar epithelial cells and was purchased from ATCC (ATCC® CCL-185, American Type Culture Collection, Manassas, VA, US). The cells were maintained in OptiMEM medium (Gibco, Life Technologies, Monza, Italy) supplemented with 10 % fetal bovine serum (FBS; Gibco) and antibiotics (penicillin/streptomycin, 100 U/mL) (Euroclone, Pero, Italy) at 37 °C in a 5 % CO_2 humidified atmosphere. Heat-inactivated SARS-CoV-2 was purchased from ATCC (VR1986HK).

For experiments, cells were seeded and grown up for 24 h in OptiMEM medium with 10 % FBS. The day after, the culture medium was replaced with OptiMEM medium with 1 % FBS, to reduce particle-FBS interactions, and $PM_{2.5}$ suspension was added directly to it to obtain the concentration of exposure and for the different exposure times. Cells were exposed also to 10 μg/mL Lipopolysaccharides, from *Escherichia coli* O111:B4 (LPS, Sigma Aldrich, Saint Louis, MO, USA) as positive control for inflammatory responses and to set-up of the experimental model.

Cells were exposed to SARS-CoV-2 viral particles depending on the different biological endpoints investigated. Viability, cytokines release, gene expression and protein analysis were analyzed after 72 h of exposure to $PM_{2.5}$, SARS-CoV-2, and PM+SARS-CoV-2 (cells simultaneously exposed to airborne and viral particles). Endosomal markers (RAB5 and RAB7 expression) and cell ultrastructure analysis were performed on the following treatment: cells exposed only to $PM_{2.5}$ for 72 + 2 h (PM), cells primed with $PM_{2.5}$ for 72 h and then exposed to viral particles for additional 2 h (PM+SARS) and cells left in culture unexposed for 72 h and then exposed to SARS-CoV-2 for additional 2 h (Control+SARS). RAB5 and RAB7 were measured also on cells exposed only to SARS-CoV-2 for 72 + 2 h (SARS) to assess if a prolonged exposure to SARS may activate the endocytic pathway. Cytokines release, gene expression and protein analysis were studied also on cell exposed to $PM_{2.5}$ and SARS-CoV-2 for 72 + 24 h, i.e. cells primed with PM for 72 h and then exposed to SARS-CoV-2, without removing PM, for additional 24 h (PM+SARS) and on cells left in culture for 72 h and then exposed to viral particles for the last 24 h (Control+SARS).

All in vitro experiments were evaluated in three independent biological replicates.

2.6. Cell viability

The viability of cells exposed to $PM_{2.5}$ and/or SARS-CoV-2 particles was assessed by means of Alamar Blue assay (Life Technologies, Monza, Italy) accordingly to the manufacturer's instruction.

Depending on the incubation time, A549 cells were seeded at different densities (2×10^4 cell/cm^2 for 24 h of exposure, 1×10^4 cell/cm^2 for 48 h and 5×10^3 cell/cm^2 for 72 h) and exposed to particles after 24 h. For set-up experiments, cells were also exposed to different $PM_{2.5}$ concentrations (1, 2.5, 5, 7.5 and 10 μg/cm^2) for 24, 48 and 72 h. Cells were also exposed for 72 h to different SARS-CoV-2 concentrations (1.2×10^2, 2.5×10^2, 3.8×10^2, 5×10^2 and 6.3×10^2 genome copies/cm^2) to select the optimal condition for experiments with viral particles (see

Supplementary data 1).

After treatment, a solution containing 1:10 of Alamar Blue reagent and OptiMEM medium with 10 % FBS was added into each well for 3 h. After incubation, the absorbance of each sample was read to the spectrophotometer (Infinite 200 Pro, TECAN, Männedorf, Switzerland) at 570 nm and compared to control values.

The relative viability [%] related to the control samples (untreated cells) was calculated according to the formula:

$$\text{Cell viability} = (\text{ODsample}/\text{ODcontrol}) \times 100$$

Results reported as percentage of viable cells are expressed as mean ± SEM of viable cells in comparison to the controls (untreated cells).

2.7. Pro-inflammatory cytokines release

The protein levels of IL-6 and IL-8 considered as representative of the inflammatory response were analyzed by ELISA matched antibody pair kit (Invitrogen, Life Technologies, Monza, Italy) in the supernatants collected at the end of the different exposures.

At the end of treatments, cell culture supernatants were recovered from exposed and control cells and centrifuged at 12000 rpm for 6 min at 4 °C to remove debris and floating cells. The resulting supernatants were collected and stored at minus 80 °C until protein analysis.

ELISA was performed according to the manufacturer's instructions. The absorbance of each sample was measured by a multiplate reader (Infinite 200 Pro, TECAN) at 450 and 630 nm and the pg/mL of released pro-inflammatory proteins was calculated based on a standard curve.

2.8. Western blotting analysis

Cells for protein expression evaluation were seeded into 6-well plates at a concentration of 5×10^3 cells/well and exposed to $PM_{2.5}$ (2.5 μg/cm^2) and SARS-CoV-2 (2.5×10^2 genome copies/cm^2) for the selected exposure times (72 h, 72 + 2 and 72 + 24 h). At the end of exposure, cells were lysed on ice in RIPA buffer (150 mM NaCl, 1 % Triton X-100, 0.5 % sodium deoxycholate, 0.1 % SDS, 50 mM Tris pH 8.0) and 0.1 % of proteases inhibitor, added just before use. The total protein content was measured by the Bicinchoninic Acid Protein assay kit (Sigma Aldrich, Milano, Italy) according to the manufacturer's instructions. Equal amounts of proteins were loaded onto 10 % SDS-PAGE (Sodium Dodecyl Sulphate - PolyAcrylamide Gel Electrophoresis) gels, separated and finally transferred on nitrocellulose membranes. Membranes were incubated for 1 h with blocking buffer (TBS + 0.1 % Tween20 + 5 % (*w/v*) BSA). Afterward, membranes were incubated at 4 °C overnight (O/N) with the following primary antibodies (diluted according to datasheets): ACE2, RAB5, RAB7 (Invitrogen, Life Technologies), NF-κB p65 and HO-1 (Cell Signaling Technology, Danvers, USA). β-actin was used for loading control (Cell Signaling Technology, USA). The following day, membranes were incubated with the specific HRP-linked secondary antibodies (anti-rabbit and anti-mouse IgG, 1:2000, Cell Signaling) for 1 h at room temperature (RT). Finally, proteins were detected by enhanced chemiluminescent (ECL, Euroclone) and digital images taken by means of a luminescence reader (Biospectrum-UVP, LLC, Upland, CA, United States). The densitometry analysis was performed with dedicated software (VisionWorks LS).

2.9. Gene expression

Cells for RNA analysis were seeded into 6-well plates for the selected exposure times (72 h and 72 + 24 h). At the end of exposure, cells were collected, centrifuged and the pellet resuspended in RNA Lysis Buffer and stored at minus 80 °C until RNA isolation. Monarch Total RNA Miniprep Kit (New England Biolabs, Euroclone) was used to extract total RNA from cells, according to the manufacturer's instructions. Total RNA samples were treated with DNase I - RNase-free to remove genomic DNA contamination. One μg of RNA was reverse transcribed with LunaScript RT SuperMix Kit (New England Biolabs, Euroclone). Gene expression analysis was performed by real-time PCR. PCR reactions were run on QuantStudio 3 Real-Time PCR System (Applied Biosystems, Life Technologies) using Luna Universal qPCR Master Mix (New England Biolabs, Euroclone) and the following program: initial denaturation at 95 °C for 60 s, then 40 cycles of 95 °C for 15 s and 60 °C for 30 s, followed by a melting curve. The amount of target cDNA in each sample was calculated by the ΔΔCt method, normalized to the expression of a reporter gene, and expressed as $\log_2$ of the fold change relative to control cells. As reference genes, STBD and β-Actin were used. The complete list of genes and primer sequences is reported in Supplementary data 2.

2.10. Cell ultrastructure analysis

For TEM analysis, cells cultured in 6-well plates as described above, were trypsinized, washed in PBS, and immediately fixed for 60 min at RT in a 2 % glutaraldehyde fixative solution prepared in the same medium. Subsequently, cells were centrifuged for 10 min at 13200 rpm to obtain a pellet, and fixative solution was replaced with 2 % glutaraldehyde and 2 % paraformaldehyde solution prepared in 0.1 M phosphate buffer (PB). After 1 h of fixation, cell pellets were washed with PB 0.1 M and post-fixed for 1 h in 1 % Osmium Tetroxide solution prepared in PB 0.1 M at 4 °C in the dark. After several washes in PB 0.1 M, samples were dehydrated in an ascending ethanol series, transferred in a final concentration of propylene oxide, and then embedded in Epon resin. After resin polymerization at 60 °C for 48 h, samples were cut with Rickert-Jung ultramicrotome, and ultra-thin sections were collected on TEM grids. Ultrathin sections (50-70 nm) were stained with uranyl acetate and lead citrate solutions. Samples were observed with a JEM 2100 Plus Transmission Electron Microscope (JEOL, Japan), operating at 80 kV acceleration voltage and equipped with an 8-megapixel (Gatan, US) Rio complementary metal-oxide-superconductor (CMOS) camera.

2.11. Statistical analysis

Data are presented as Mean and Standard Error of Mean (SEM) of three independent experiments. Statistical analyses were performed using GraphPad Prism 6 software, using One-way or Two-way ANOVA with Dunnett's post hoc multiple comparisons tests. Values of $p < 0.05$ were considered statistically significant.

3. Results

3.1. Particles characterization

Shape and state of aggregation of particles were analyzed by TEM. $PM_{2.5}$ presents aggregates of nanometric electron-dense particles (up to 50 nm for each primary particle and aggregates of a few hundreds of nm, up to few micrometers), typical of soot emissions from combustion processes (Fig. 1A, B, C). The morphology of SARS-CoV-2 was also characterized by negative staining. The virions display a spherical shape and a diameter of approximately 80-90 nm (Fig. 1D, E, F).

The chemical composition was determined by characterizing the total carbon (TC), inorganic ions (Table 1) and metals and trace elements (Table 2). The main polycyclic aromatic hydrocarbons (Table 3) were also characterized, as organic species.

Water-soluble inorganic ions represented the major chemical fraction of $PM_{2.5}$ collected in Milan during winter 2021. As typical of the winter season, Nitrate was the most abundant (Table 1). The lowest concentrations were found for Calcium and Magnesium.

Table 2 reports the elements detected by XRF. From that table, it is evident that S, K, Cl were the dominant elements, followed by Na and Fe. The minimum concentrations were observed for Cu, Co, Cd and As.

Table 3 summarizes the Polycyclic Aromatic Hydrocarbons (PAHs) content (ng/μg) of the $PM_{2.5}$ samples. PAHs represent an important toxicological class of chemicals in the organic fraction. The sum of the

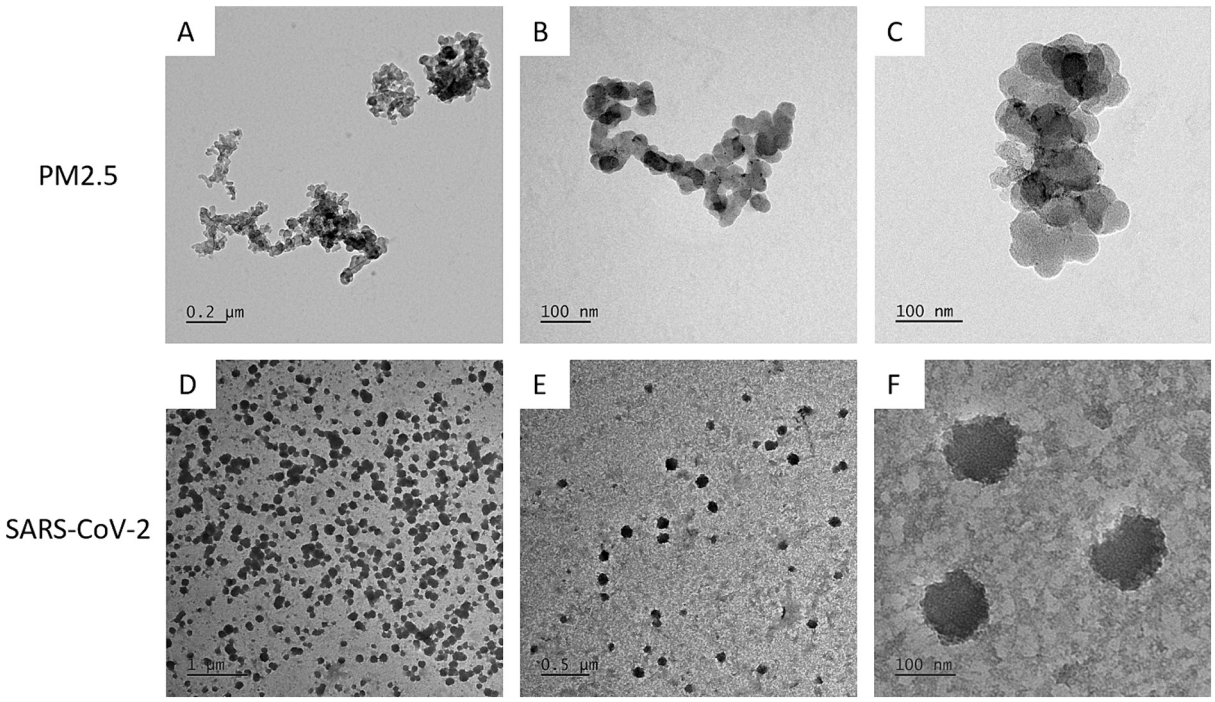

Fig. 1. TEM pictures of $PM_{2.5}$ and SARS-CoV-2 suspensions. Typical soot-like aggregations of nanometric carbonaceous particles are evident as expected for the urban source of fine PM (A, B, C). SARS-CoV-2 virions are well recognizable with a diameter in the order of 100 nm (D, E, F).

Table 1
Relative mass (expressed as mg of chemical species/mg of PM) for TC, IC, and ionic species in $PM_{2.5}$ collected during winter 2021. Organic species (TC) and ionic ones (specifically nitrates) are explaining the majority of the sampled mass, as expected from a winter urban PM sample collected in the Po valley.

Main PM components	Relative mass (mg/mg of PM)	Standard deviation (mg/mg of PM)
TC[a]	0.593	0.112
Chloride	0.015	0.007
Nitrate	0.621	0.265
Sulfate	0.071	0.035
Sodium	0.017	0.012
Ammonium	0.132	0.054
Potassium	0.036	0.016
Magnesium	0.001	0.000
Calcium	0.003	0.002
Not explained mass	0.215	0.183

[a] Inorganic carbon was always under the LOQ.

16 analyzed PAHs (expressed as the average of four independent replicates) was 66.7 ± 38 ng/µg. It can be noticed that 5- and 6 rings PAHs, such as benzo[*b*]fluoranthene, benzo[*k*]fluoranthene, benzo[*ghi*]perylene, indeno[1,2,3-*cd*]pyrene and benzo[*a*]pyrene, were the most abundant compounds.

3.2. $PM_{2.5}$ exposure concentration tests

In the present study, a single sub-toxic $PM_{2.5}$ concentration of 2.5 µg/cm^2 was selected for in vitro investigations. To determine it, a time- and dose-response study of PM-induced toxicity was preliminary performed on A549 cells. None of the treatments produced significant alterations in cell viability when compared to the corresponding control except for cells exposed to PM for 72 h to 10 µg/cm^2 (Fig. 2A).

As a measure of PM-induced pro-inflammatory effects, the release of IL-8 was measured after 24, 48 h and 72 h of exposure. After 72 h, a weak secretion of IL-8 was found only on cells exposed to 2.5 µg/cm^2 PM (see Supplementary data 3). The level of NF-kB p65 in cell lysates was also measured in cells exposed to the lower PM concentrations (1 and 2.5 µg/cm^2) for 72 h using an InstantOne ELISA kit. Results confirmed that inflammatory response is slightly modulated only after exposure to 2.5 µg/cm^2 of $PM_{2.5}$ (see Supplementary data 3). Considering these results, the exposure concentration of 2.5 µg/cm^2 was retained as the one avoiding cell death and ensuring the activation of the inflammatory pathway of interest.

To confirm the activation of the inflammatory response, we

Table 2
Relative content of metals/trace elements in $PM_{2.5}$ collected during winter 2021 (ng/µg).

Metals and trace elements	Relative content (ng/µg of PM)	Standard deviation (ng/µg of PM)
Na	7.80	7.56
Mg	2.67	2.39
Al	1.86	1.70
Si	4.59	3.39
K	19.56	14.72
Cu	ND	ND
Ca	4.02	3.61
Ti	0.26	0.25
V	0.03	0.03
Cr	0.12	0.09
Mn	0.41	0.36
Fe	6.13	6.90
Co	0.00	0.00
Ni	0.05	0.06
Zn	1.99	2.20
As	0.02	0.02
Br	0.49	0.58
Rb	0.20	0.11
Pd	0.61	0.76
Sb	0.19	0.14
Ba	2.35	1.66
Pb	0.46	0.56
Cd	ND	ND
Cl	13.95	16.85
S	28.12	26.08
Σ metals and trace elements (µg)	95.87	90.03

Table 3
Relative content of Polycyclic Aromatic Hydrocarbons (PAHs) in $PM_{2.5}$ collected during winter 2021 (ng/μg). nd = not detected.

PAHs	Relative content (ng/μg of PM)	Standard deviation (ng/μg of PM)
naphthalene	nd	nd
acenaphthylene	nd	nd
acenaphthene	0.456	0.128
fluorene	0.097	0.044
phenanthrene	1.57	0.581
anthracene	0.17	0.05
fluoranthene	2.91	1.20
pyrene	3.57	1.41
benzo[*a*]anthracene	2.81	1.32
chrysene	5.85	2.58
benzo[*b*]fluoranthene	10.60	6.25
benzo[*k*]fluoranthene	9.40	6.22
benzo[*a*]pyrene	7.96	4.91
indeno[1,2,3-*cd*]pyrene	9.42	6.73
dibenz[*a,h*]anthracene	1.89	1.38
benzo[*ghi*]perylene	10.0	6.17

The endotoxin levels in PM-extracted samples were also measured. Results showed that $PM_{2.5}$ samples at the concentration of 25 μg/mL contained about 6.6 ± 0.56 EU/mg of PM.

measured ACE2 protein expression (Fig. 2B) and cytokines release (IL-8 and IL-6, Fig. 2C and D) at 24, 48 and 72 h of exposure to the selected concentration of $PM_{2.5}$ (2.5 μg/cm^2) compared to parallel exposure of cells to LPS (10 μg/mL), used as a positive control.

Results showed that $PM_{2.5}$ induces a time-dependent increase in ACE2 (Fig. 2B) and IL-6 levels (Fig. 2D), although not significantly. LPS, as expected, induced a significant IL-6 secretion at all the time points investigated. IL-8 was instead increased by LPS treatment only after 72 h of exposure (Fig. 2C).

Considering these results, we selected 72 h of exposure at 2.5 μg/cm^2 as the time point of interest for subsequent experiments.

Similarly, tests with SARS-CoV-2 were performed to define an appropriate exposure concentration, considering cell viability and inflammatory response (IL-8 release) as the endpoint of interest (see Supplementary data 1). 2.5 × 10^2 genome copies/cm^2 was defined as SARS-CoV-2 concentration for the subsequent experiments.

3.3. $PM_{2.5}$ and SARS-CoV-2 combined effects on lung cells: inflammation and oxidative stress

The combined effects of $PM_{2.5}$ and SARS-CoV-2 simultaneously added to the cell culture were tested to assess the possibility that airborne particles might play a role in facilitating viral infection.

Cells were exposed to PM (2.5 μg/cm^2) or SARS-CoV-2 (2.5 × 10^2 genome copies/cm^2) alone and to PM and SARS added simultaneously (PM&SARS) for 72 h. None of the treatments produced significant alterations in cell viability (Fig. 3A) when compared to the relative control (not exposed cells).

Protein expression of ACE2, NF-kB and HO-1, as key markers of the inflammatory status and the oxidative stress response, were then investigated. PM exposure (also in combination with SARS) promoted a statistically significant increase in the expression of the anti-inflammatory marker ACE2, when compared to the control, while SARS alone was not able to promote such increase (Fig. 3B), confirming the importance of PM exposure to increase ACE2 expression and supporting that ACE2 is not altered by the viral infection.

NF-kB was found to be increased, although not significantly, by PM

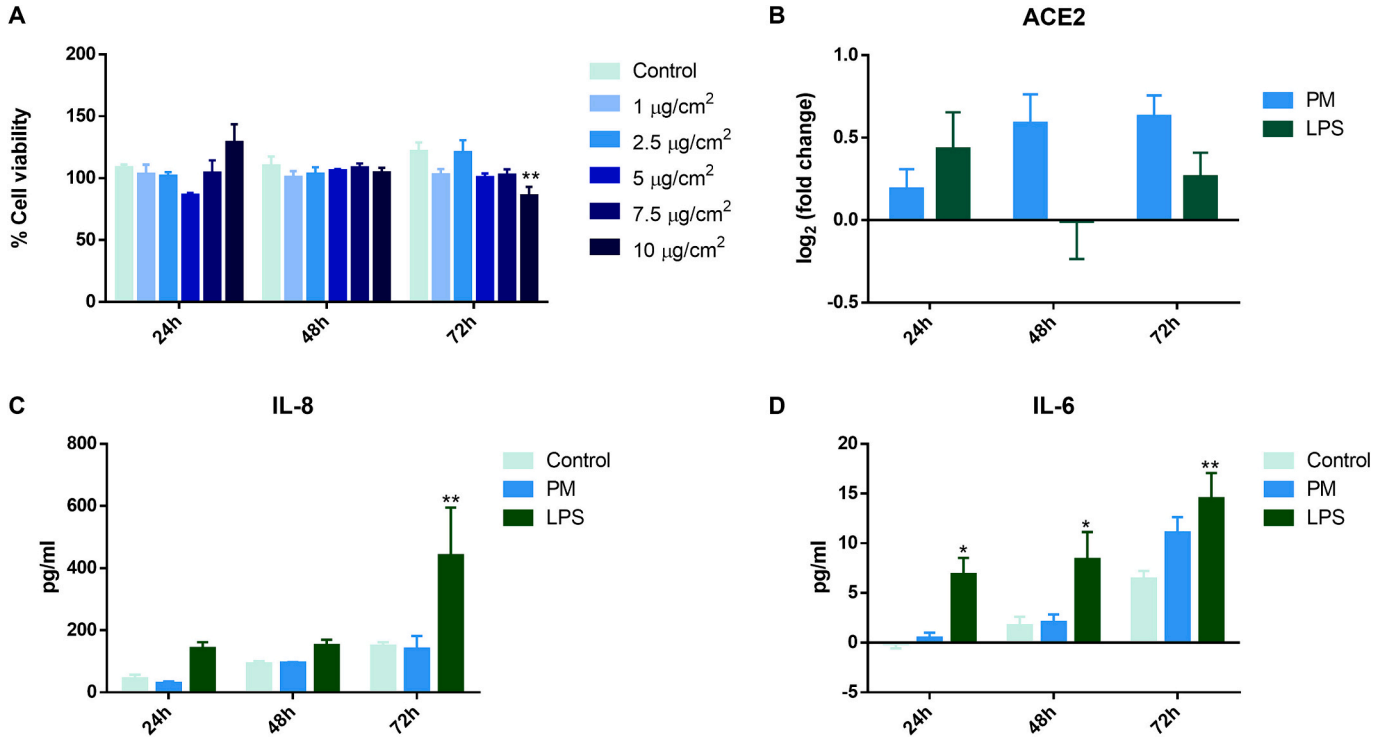

Fig. 2. $PM_{2.5}$ exposure concentration experiments. A) Alamar Blue assay. A549 cell viability was evaluated after 24, 48 and 72 h of exposure to increasing $PM_{2.5}$ concentrations (1, 2.5, 5, 7.5 and 10 μg/cm^2). Histograms show the percentage of viable cells compared to the control (unexposed) cells. Each bar shows mean ± SEM of three independent experiments ($N = 3$). Statistical analysis was performed by Two-way ANOVA with Dunnett's multiple comparisons tests. $^{**}p < 0.01$ vs control cells. B) ACE2 protein expression in A549 cells after 24, 48 and 72 h of A549 exposure to 2.5 μg/cm^2 $PM_{2.5}$ and 10 μg/mL LPS (positive control). Bars represent the mean ± SEM of three independent experiments ($n = 3$). Control value (i.e., lung cells not exposed to PM nor to SARS-CoV-2) is equal to zero having considered the $\log_2$ of the fold change. C, D) Pro-inflammatory response. IL-8 (C) and IL-6 (D) protein secretion after 24, 48 and 72 h of A549 exposure to 2.5 μg/cm^2 $PM_{2.5}$ and 10 μg/mL LPS (positive control). Each bar shows mean ± SEM of three independent experiments ($N = 3$). Statistical analysis was performed by Two-way ANOVA with Dunnett's multiple comparisons tests. $^{**}p < 0.01$ and $^{*}p < 0.05$ vs control cells.

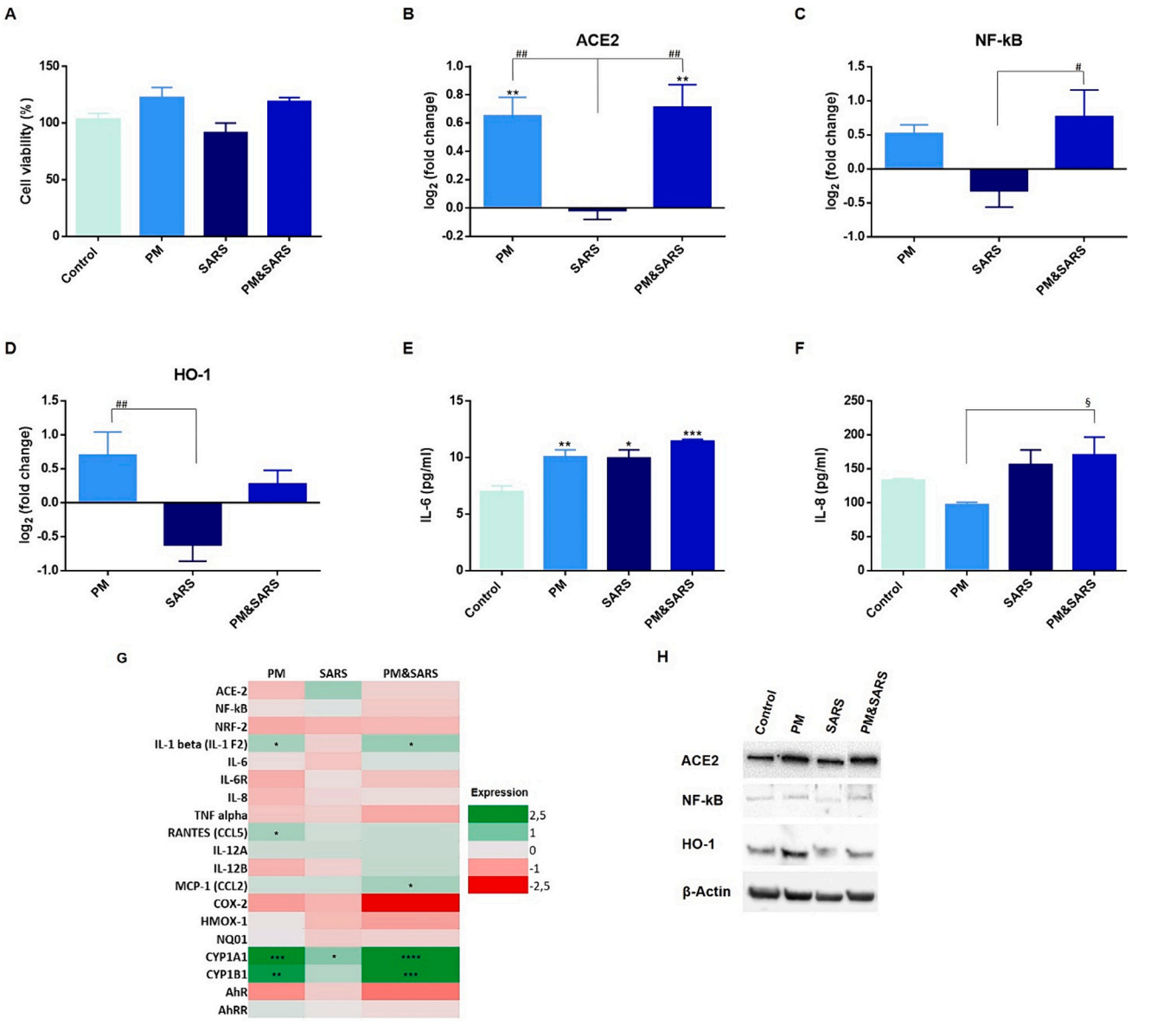

Fig. 3. Cell viability and protein and gene expression in A549 cells exposed to $PM_{2.5}$ and SARS-CoV-2 for 72 h. A) Cellular metabolic activity assessed by Alamar Blue assay. Histograms show the percentage of viable cells compared to the unexposed control cells. Each bar shows mean ± SEM of three independent experiments ($N = 3$). Statistical analysis was performed by One-way ANOVA with Dunnett's multiple comparisons test. B, C, D) ACE2 (B), NF-kB (C) and HO-1 (D) protein expression. Bars represent the mean ± SEM of three independent experiments ($n = 3$). Control value (i.e., lung cells not exposed to $PM_{2.5}$ nor to SARS-CoV-2) is equal to zero having considered the $\log_2$ of the fold change. Statistical analysis was performed by One-Way ANOVA with Dunnett's multiple comparison test. $^{**}p < 0.01$ vs control cells. $^{\#\#}p < 0.01$, $^{\#}p < 0.05$ vs SARS exposed cells. E, F) Pro-inflammatory response. IL-6 (E) and IL-8 (F) protein secretion. Each bar shows mean ± SEM of three independent experiments (N = 3). Statistical analysis was performed by One-way ANOVA with Dunnett's multiple comparisons tests. $^{***}p < 0.001$, $^{**}p < 0.01$ and $^{*}p < 0.05$ vs control cells. $^{\S}p < 0.05$ vs PM&SARS exposed cells. G) Gene expression analysis. Modulation of genes related to inflammation, oxidative stress, and oxidation by cytochrome P450. Control value (i.e., lung cells not exposed to $PM_{2.5}$ nor to SARS-CoV-2) is equal to zero having considered the $\log_2$ of the $^{2\text{-}\Delta\Delta Ct}$. Changes in gene expression, increased (green), decreased (red) or equal (gray) compared to the unexposed control cells are reported. Statistical analysis was performed by One-way ANOVA with Dunnett's multiple comparisons tests. $^{****}p < 0.0001$, $^{***}p < 0.001$, $^{**}p < 0.01$ and $^{*}p < 0.05$ vs control cells. H) Representative images of Western Blot bands.

and PM&SARS samples. SARS exposure determined a reduced expression of the protein statistically different from PM&SARS cells (Fig. 3C). HO-1 protein levels were also examined. While PM and PM&SARS samples slightly augmented the protein release, no effects were induced by solely SARS. Moreover, PM sample induced a statistically significant increase of the protein when compared to SARS alone (Fig. 3D).

The inflammatory response was also explored, by measuring the secretions of IL-6 and IL-8. IL-6 release significantly increased with all treatments (Fig. 3E). On the other hand, IL-8 secretion was found slightly modulated only after the co-exposure PM&SARS. Interestingly, IL-8 released was significantly increased after the co-exposure PM&SARS compared to PM samples (Fig. 3F) supporting the evidence of a combined effects of PM and SARS in inducing an increased inflammatory response.

Considering the previous results, a panel of selected genes related to inflammatory response, oxidative stress, and metabolism by cytochrome P450 has been screened to go deeper into the cell mechanisms possibly involved in the combined effects of $PM_{2.5}$ and SARS-CoV-2 to be exploited in the next studies. Based on the gene expression analysis (Fig. 3G), treatment with PM induced an increased expression of IL-1β,

RANTES, CYP1A1 and CYP1B1 gene transcripts, while SARS alone significantly up-regulated only CYP1A1. Besides, ACE2 gene transcript was found to increase, although not significantly. As shown in Fig. 3G, co-exposure PM&SARS promoted a significant increase in IL-1β, MCP-1, CYP1A1 and CYP1B1 gene transcripts. The same genes are upregulated already by exposure to PM alone. Therefore, the results suggest that the combined exposure to PM&SARS is not determining a specific pattern of genes activation, but rather the co-exposure reinforces (as suggested by the stronger *p*-values) the effects determined by $PM_{2.5}$ exposure.

3.4. $PM_{2.5}$ as favoring agent to SARS-CoV-2 internalization

To get more information on the mechanisms by which $PM_{2.5}$ favors viral internalization of SARS-CoV-2, we performed experiments to verify the exploitation of the endosomal pathway. Thus, the protein expression of the endosomal early RAB5 (Fig. 4A) and late RAB7 (Fig. 4B) markers was measured.

Lung cells were exposed to PM or SARS for 72 h or left in culture without treatment (control cells). After 72 h SARS-CoV-2 was added to PM and control cells for 2 additional hours of exposure (Control+SARS and PM+SARS samples), similarly the treatment with PM or SARS alone were prolonged for 2 additional hours.

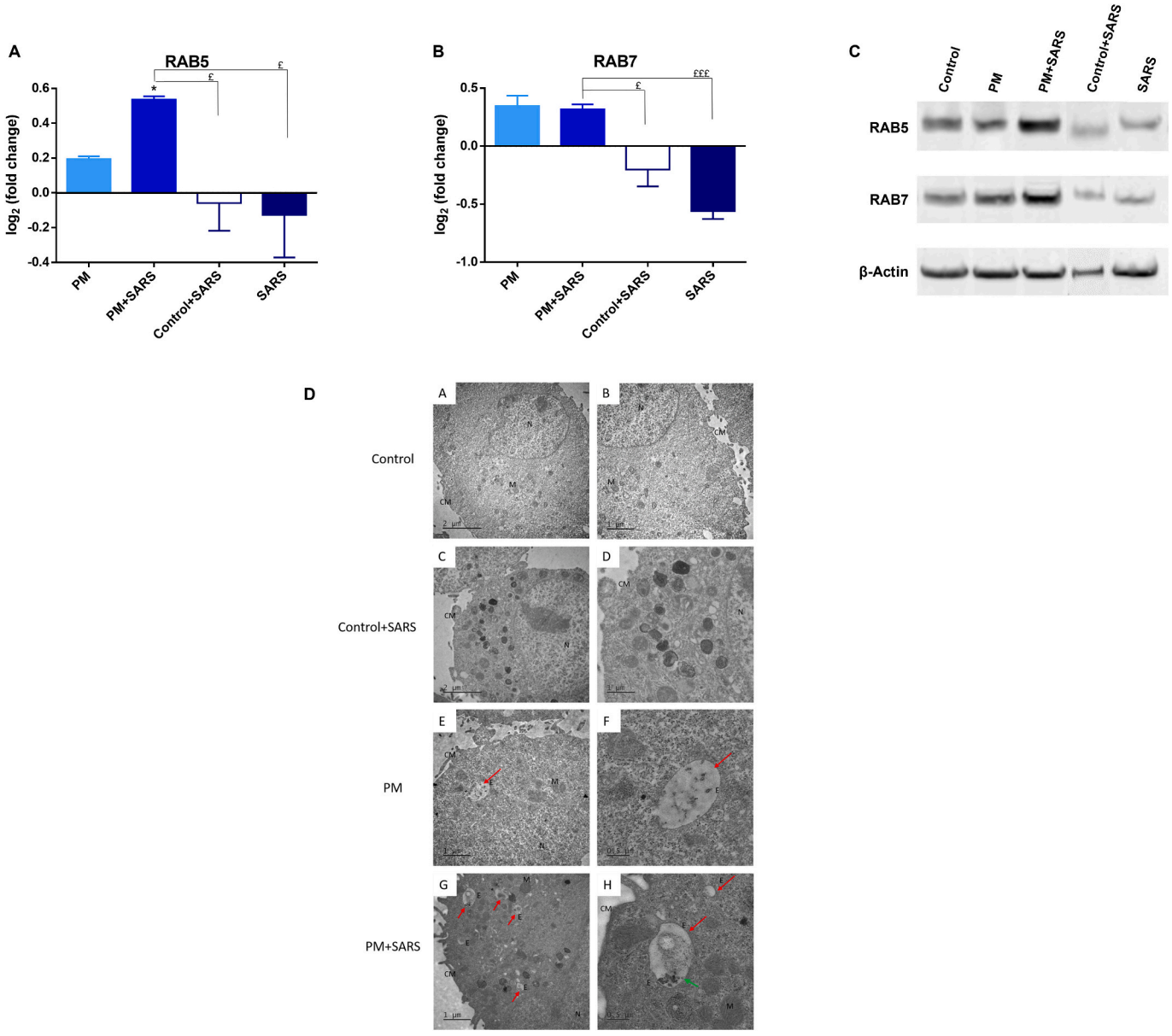

Fig. 4. Protein expression and electron microscopy analysis on A549 cells exposed to $PM_{2.5}$ and SARS-CoV-2 for 72 + 2 h. RAB5 (A) and RAB7 (B) protein expression in A549 cells primed with $PM_{2.5}$ (2.5 μg/cm^2) for 72 h and exposed to SARS-CoV-2 (2.5 × 10^2 genome copies/cm^2) for 2 additional hours. Bars represent the mean ± SEM of three independent experiments ($n = 3$). Control value (i.e., lung cells not exposed to $PM_{2.5}$ nor to SARS-CoV-2) is equal to zero having considered the $\log_2$ of the fold change. Statistical analysis was performed by One-Way ANOVA with Dunnett's multiple comparison test. $^*p < 0.05$ vs control cells. $^{£££}p < 0.1$ and $^{£}p < 0.05$ vs PM+SARS exposed cells. C) Representative images of Western Blot bands. D) TEM images of A549 cells primed with $PM_{2.5}$ (2.5 μg/cm^2) for 72 h and exposed to SARS-CoV-2 (2.5 × 10^2 genome copies/cm^2) for 2 additional hours. Panels A, B) Control cells; Panels C, D) Control cells left in culture without treatment for 72 h and then treated with SARS-CoV-2 for additional 2 h; Panels E, F) Cells exposed only to $PM_{2.5}$; Panels G, H) Cells exposed to $PM_{2.5}$ for 72 h and then treated with SARS-CoV-2 for additional 2 h. Endosomal vesicles are present in the cell cytoplasm, many of which contain particles. CM = cell membrane; N = nucleus, M = mitochondria; E = endosome. Red arrows show particles inside cells. Green arrow shows viral particles in the endosomes.

PM alone induced a slight not significant increase in the endosomal markers here investigated while exposure to SARS-CoV-2 alone induced a slight not significant downregulation of the pathway. Significantly, cells primed with PM (therefore with increased expression of ACE2) and then exposed to SARS-CoV-2 for additional 2 h, showed a significant increase in RAB5 expression suggesting that, after exposure to PM, the virus is more easily internalized into cells. The enhanced capability of internalization was not found in control cells exposed to SARS for 2 additional hours (Control+SARS sample, Fig. 4A). PM and PM+SARS cells induced a moderate increase of the RAB7 protein, although not significant (Fig. 4A) if compared to control cells while in Control+SARS and SARS exposed cells a moderate not significant decrease of the protein was measured (Fig. 4B). A significant difference was observed comparing PM and PM+SARS versus Control+SARS and SARS (Fig. 4B)

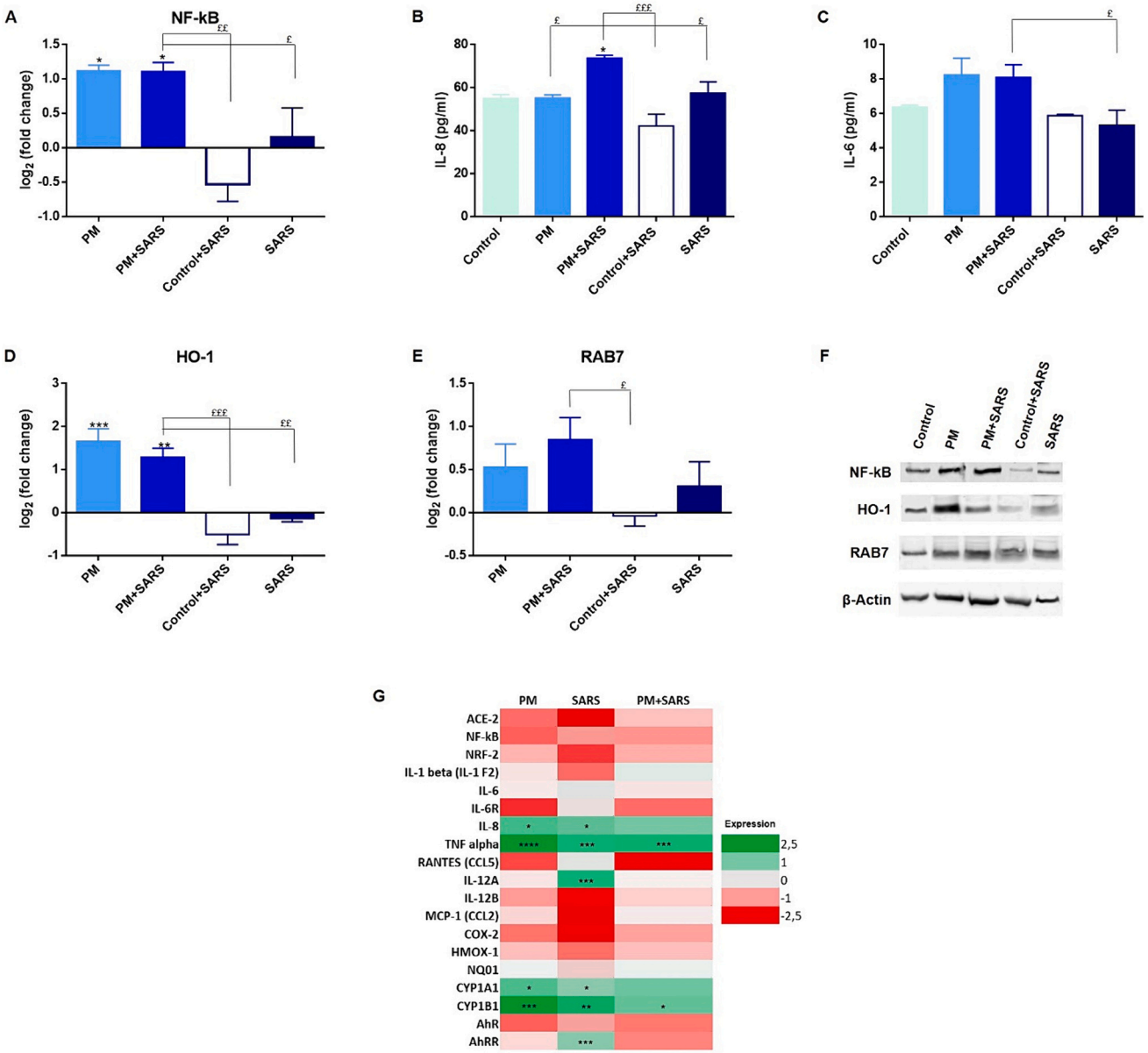

Fig. 5. Protein and gene expression in A549 cells exposed to $PM_{2.5}$ and SARS-CoV-2 for 72 + 24 h. A) NF-kB protein expression on cells exposed to $PM_{2.5}$ and SARS-CoV-2 for 72 + 24 h. Bars represent the mean ± SEM of three independent experiments ($n = 3$). Control value (i.e., lung cells not exposed to $PM_{2.5}$ nor to SARS-CoV-2) is equal to zero having considered the $\log_2$ of the fold change. Statistical analysis was performed by One-Way ANOVA with Dunnett's multiple comparison test. $^{*}p < 0.05$ vs control cells. $^{\text{££}}p < 0.01$ and $^{\text{£}}p < 0.05$ vs PM+SARS exposed cells. B, C) Pro-inflammatory response. IL-8 (B) and IL-6 (C) protein secretion. Each bar shows mean ± SEM of three independent experiments ($N = 3$). Statistical analysis was performed by One-way ANOVA with Dunnett's multiple comparisons tests. $^{*}p < 0.05$ vs control cells. $^{\text{£££}}p < 0.001$ and $^{\text{£}}p < 0.05$ vs PM+SARS exposed cells. D) HO-1 protein expression. Bars represent the mean ± SEM of three independent experiments (n = 3). Control value (i.e., lung cells not exposed to PM nor to SARS-CoV-2) is equal to zero having considered the $\log_2$ of the fold change. Statistical analysis was performed by One-Way ANOVA with Dunnett's multiple comparison test. $^{***}p < 0.1$ and $^{**}p < 0.01$ vs control cells. $^{\text{£££}}p < 0.001$ and $^{\text{££}}p < 0.01$ vs PM+SARS exposed cells. E) RAB7 protein expression. Bars represent the mean ± SEM of three independent experiments (n = 3). Control value (i.e., lung cells not exposed to $PM_{2.5}$ nor to SARS-CoV-2) is equal to zero having considered the $\log_2$ of the fold change. Statistical analysis was performed by One-Way ANOVA with Dunnett's multiple comparison test. $^{\text{£}}p < 0.05$ vs PM+SARS exposed cells. F) Representative images of Western Blot bands. G) Gene expression analysis. Control value (i.e., lung cells not exposed to PM nor to SARS-CoV-2) is equal to zero having considered the $\log_2$ of the $^{2\text{-}\Delta\Delta Ct}$. Changes in gene expression, increased (green), decreased (red) or equal (gray) compared to the unexposed control cells are reported. Statistical analysis was performed by One-way ANOVA with Dunnett's multiple comparisons tests. $^{****}p < 0.0001$, $^{***}p < 0.001$, $^{**}p < 0.01$ and $^{*}p < 0.05$ vs control cells.

suggesting again a different activation of the endosomal pathway in cells primed with PM or not prior to the exposure to the viral particles.

In support of the results obtained, electron microscopy experiments were also performed to verify the internalization of the viral particles in the alveolar cells (Fig. 4C). The ultrastructural analysis of cells exposed to particles shows that the treatment PM+SARS increased the intracellular formation of endosomal vesicles (Fig. 4C, Panels G, H), compared to cells exposed only to $PM_{2.5}$ (Fig. 4C, Panels E, F). In panels F and H large endosomes containing particles are evident. Interestingly, in panel F particles have shape and dimensions in agreement with those of the viral particles presented in Fig. 1E suggesting the internalization of viral particles in the endosomes.

3.5. $PM_{2.5}$ as a factor increasing the responses to SARS-CoV-2 infection

The possibility that cells pre-activated with $PM_{2.5}$ could be more sensitive to SARS-CoV-2 infection was then explored. Cells primed with PM, SARS or left unexposed (control cells) for 72 h were additionally exposed for 24 h to SARS-CoV-2.

NF-kB expression and cytokines release were measured to assess the inflammatory response. Exposure to PM or to PM+SARS induced a significant increase in NF-kB when compared to control cells. On the contrary, viral particles alone (SARS-exposed cells) were unable to modulate the protein expression (Fig. 5A). Notably, IL-8 was found significantly increased only in PM+SARS cells (Fig. 5B). The difference was statistically relevant also comparing PM+SARS to PM, Control+SARS and SARS exposed cells, thus suggesting that the co-presence of PM and SARS facilitate the increase in the inflammatory response. IL-6 was slightly released in PM and PM+SARS exposed cells compared to control. A significant difference was observed comparing PM+SARS and SARS samples (Fig. 5C).

HO-1 protein expression, measured as a marker of oxidative processes, was significantly increased in cells exposed to PM and PM+SARS. Control+SARS and SARS treatments were unable to modulate the protein expression, confirming again that the oxidative pathway, if activated, is related mainly to PM exposure (Fig. 5D). RAB7 protein was found increased, although not significantly in PM and PM+SARS samples. Moreover, a statistical difference was found comparing PM+SARS and Control+SARS exposed cells (Fig. 5E).

Finally, the same panel of genes investigated on the cells exposed for 72 h was analyzed. As shown in Fig. 5F few genes were found up-regulated at this time of exposure. The PM+SARS exposed cells showed a statistically significant upregulation of TNF-α and CYP1B1 genes. These increases were observed also in the PM and SARS exposed cells. Moreover, PM and SARS also increased the gene expression of IL-8 and CYP1A1, with SARS also increasing the expression of IL-12 A and AhRR gene transcript suggesting a specific activity of the viral particles alone, only at this late time of exposure.

4. Discussion

The dramatic impact of viral infections on human health has been demonstrated by the recent pandemic and much evidence on the effects of these viruses at cardiovascular and pulmonary levels have been reported (Groulx et al., 2018; Michaud, 2009). Moreover, air pollution has been suggested to play a role in the cardiovascular and pulmonary diseases related to pathogens infection (Domingo et al., 2020). In this context, the emergence of new viruses requires a deeper understanding of the close relationship among airborne pollutants and viral pathogens, with a focus on the pathogenic mechanisms involved, to improve the prevention and treatment of potentially exposed populations. Today, data on the joint toxicity of environmental pollutants and viral pathogens are very limited.

In a previous study, the contribution of $PM_{2.5}$ exposure in increased susceptibility to SARS-CoV-2 infection and inflammatory outcomes has been suggested (Marchetti et al., 2023), showing the importance to study the in vitro toxicological responses in lung epithelial cells.

Here, we report an investigation into the various cyto-toxicological properties of $PM_{2.5}$ and SARS-CoV-2, with particular attention to how the toxic effects might change with the co-presence of PM and viral particles.

It is known that size, structure, and chemical composition of particles are associated with their toxicological properties and influence their residence time in the atmosphere and their deposition within the respiratory system (Kelly and Fussell, 2012). TEM analysis provided information about particle dispersion and shape and revealed that particles are smaller than 0.1 μm (according to the 2.5 μm cut-off head used to sample PM) and tend to form agglomerates accordingly to the primary urban emissions (mainly road traffic) of the sampling site. Accordingly, our samples are composed primarily of total carbon (TC) and inorganic ion nitrate, as representative of secondary aerosol. They resulted also enriched in crustal elements (such as Al, Si, K, Ca, and Fe). The determination of PAH concentrations revealed a high content of 5- and 6- rings PAHs. The results from the chemical analyses confirm previous data on the same sampling site (Gualtieri et al., 2009; Perrone et al., 2013).

For a complete characterization of the particles, we also performed an evaluation of the endotoxin content on the particle extract. Results showed that $PM_{2.5}$ samples contained about 6 EU/mg, which is consistent with our previous studies on particles collected in that area, showing that during the winter season, the $PM_{2.5}$ endotoxin content is relatively low (Gualtieri et al., 2011; Longhin et al., 2013). These results agree with literature data showing that highest peaks of endotoxin can be found during late spring/summer (Jalava et al., 2016; Ljunggren et al., 2019).

TEM analysis on SARS-CoV-2 particles confirm the typical round shape of the virions of circa 100 nm of diameter, as reported also by Nardacci et al. (2021).

The exposure concentration used here, besides being among the lowest reported in the literature for toxicological studies on PM, is also supported by previous studies (Li et al., 2003) that determined a daily potential bronchial and alveolar deposition of 2.3 and 0.05 $\mu g/cm^2$ in conditions of high exposure periods of pollution as that normally reported in Milan and the Po' Valley region in winter period (Larsen et al., 2012).

The data obtained revealed that both airborne and viral particles did not affect cell viability. Moreover, we demonstrated that exposure to a sub-toxic concentration of $PM_{2.5}$ time-dependently alters the lung defense mechanisms, thus promoting the activation of the inflammatory pathway starting from 72 h of exposure. A previous study on bronchial epithelial cells BEAS-2B also showed a dose- and time-dependent inflammatory response (gene expression and protein secretion of pro-inflammatory cytokines) on cells exposed to $PM_{2.5}$ (Cachon et al., 2014). Similar results have been reported also by other studies (Garçon et al., 2006; Michael et al., 2013). Besides, the oxidative stress response was also found activated. As expected, AhR-induced xenobiotic enzymes (CYP1A1 and CYP1B1) genes were up-regulated, in line with the chemical characterization of fine PM and its content in PAHs. The activation of CYP enzymes is not new and it is largely reported in the literature both on in vitro (Cachon et al., 2014; Dergham et al., 2012; Marchetti et al., 2019) and murine models (Ding et al., 2021; Saleh et al., 2019).

Noteworthy, cells exposed to SARS-CoV-2 viral particles alone for >72 h showed a significant up-regulation of pro-inflammatory genes (IL-8, TNF-α, IL-12 A). These results suggest that SARS-CoV-2 alone can initiate a moderate inflammatory response also considering that we used an inactivated virus. At shorter exposure times (2 or 24 h) no effects are observed. Thus, we can hypothesize that SARS alone requires a longer exposure time to modulate the biomarkers studied here. Barhoumi et colleagues demonstrated that the SARS-CoV-2 (2019-nCoV) Spike recombinant glycoprotein can promote in vitro the activation of THP-1-like macrophages, HUVECs and PBMCs, as evidenced by the increase

of proinflammatory markers, including TNF-α (Barhoumi et al., 2021). The viral particles we used are heat-inactivated and therefore not completely representative of active viruses and we account this as a possible limitation of our study. Nonetheless, Hudák et al. (2022) studied the cellular uptake of inactivated SARS-CoV-2 particles in in vitro and in vivo mouse models and demonstrated that the virus can be internalized by various tissues, including lung, and trigger proinflammatory pathways in all tissues. In line with our findings, Li and colleagues reported a time-dependent up-regulation of pro-inflammatory cytokines, including IL-8, tumor necrosis factor-α (TNF-α), CXCL10, and CCL5 in lung epithelial cells (Calu-3) infected by the SARS-CoV-2 virus isolated from the bronchoalveolar lavage fluid sample of patients (Li et al., 2020). Interestingly, the increased expression of the AhR transcriptional targets CYP1A1, CYP1B1 and AhRR was also found in cells exposed only to viral particles. Some recent studies on COVID-19 patient samples (Giovannoni et al., 2021; Shi et al., 2023) have proposed that AhR activation during a viral infection could interfere with the activation of the protective immune pathway by suppressing the production of the type I interferons (IFN-I). Giovannoni and colleagues demonstrated indeed that several coronaviruses can up-regulate AhR and related genes at different time points post-infection, thus suppressing the endogenous anti-viral response (Giovannoni et al., 2021). In the present study the induction of the phase I xenobiotic response occurred in the absence of a parallel induction of the antioxidant defense mechanism (here represented by HMOX-1, NRF-2 and NQ01 gene transcripts and HO-1 protein levels) at the time points post-exposure investigated; moreover we report a significant upregulation of the AhR repressor gene after 72 + 24 h of exposure to SARS alone supporting that viral particles alone can interfere with the detoxification pathway altering the protective cellular systems in human alveolar cells. Noteworthy, besides altering the detoxification systems, SARS in combination with PM may also sustain the activation of the inflammatory process, as evidenced by the protein and gene expression studies.

Infectious diseases are generally caused by viruses and bacteria that enter host cells for replication. Many human pathogens in fact take advantage of the endocytosis, or phagocytosis, machinery to reach the relevant intracellular compartments. Viruses, in particular, as obligate intracellular parasites, must transport their genome into the cytosol or nucleus of target cells to replicate and assemble new virus particles (Cossart and Helenius, 2014). Endocytosis is a process by which cells internalize particles or pathogenic agents through a progressive invagination of a small region of the plasma membrane that is subsequently pinched off to form a cytoplasmic vesicle. Viruses usually are internalized by attachment to the cell surface receptors, activation of specific signaling pathways, entry into the endosomal compartments and escape into the cytosol (Cossart and Helenius, 2014). SARS-CoV-2 binding to ACE2 on the airway epithelial cells has been proposed as a crucial step to start the infection. However, several mechanisms have been proposed to clarify the way SARS-CoV-2 enters cells, including cell surface fusion or endocytosis (Miao et al., 2023; Zhang et al., 2022).

To verify if SARS-CoV-2 exploits the increased expression of ACE2 in PM-exposed cells and the network of endocytic organelles to enter the cytosol, we studied two proteins typically involved in the endosomal process: RAB5 and RAB7, that are crucial for vesicle trafficking and fusion. RAB5 is mainly associated with early endosomes (EEs) while RAB7 defines late endosomes (LEs) (Cesar-Silva et al., 2022). Our results evidence that the endosomal pathway is differentially activated by particles, with airborne particles that promote only a moderate increase of RAB5. On the contrary, a significant upregulation of RAB5 is observed in $PM_{2.5}$ primed cells exposed to SARS-CoV-2 for additional 2 h, supporting an enhanced internalization of the virus. In agreement, transmission electron microscopy pictures also indicate the presence of round shaped particles into endosomes after PM priming and SARS-CoV-2 exposure. The hypothesis we propose is that the increase in the basal state of lung inflammation induced by airborne PM determines greater internalization of viral particles through the binding of SARS-CoV-2 to the overexpressed cellular receptor ACE2 and subsequent activation of endocytosis. Significantly, viral particles alone were not able to enhance ACE2 expression and exploit the endocytic process, at any time of exposure.

Our results are sustained by Atik et colleagues whose study describes that RAB5 expression is significantly increased in COVID-19 patients (Atik et al., 2022). On the contrary, we did not find an increased expression of RAB7, except in cells exposed to PM alone. This may be related to a possible alteration of the endosomal pathway, as reported also by previous studies on COVID-19 patients and COVID-19 placental tissues (Atik et al., 2022; Benarroch et al., 2021). In line with our findings, Zhang and colleagues suggest that SARS-CoV-2 is able to block the fusion of autophagosomes with lysosomes by inhibiting the binding of the protein sorting (HOPS) complex to RAB7 and then escape from degradation (Zhang et al., 2021). Therefore, while RAB5 can be considered the hallmark of SARS-CoV-2 entry into the cells, the lack of RAB7 upregulation should be considered as the indication of the virus escaping endosomal degradation. In this view, our results confirm that lung cells activated by $PM_{2.5}$ are more prone to infections without obtaining possible protection from an upregulated endosomal pathway. This negative effect of PM, as a mechanism favorable to the binding and internalization of the virus, may therefore be relevant to explain the cases of COVID-19 infections observed in highly polluted cities (Bozack et al., 2022; Coker et al., 2020).

Our findings add another piece of evidence. In fact, cells exposed to PM and SARS-CoV-2 showed a greater responsiveness after virus internalization. NF-kB is upregulated already after 24 h of SARS-CoV-2 exposure and this upregulation, initiated by PM exposure, persists after co-exposure with SARS, while SARS alone is unable to activate an increased expression. Li and colleagues suggested the key role of the NF-kB pathway in the SARS-CoV-2-induced inflammatory responses (Li et al., 2020). The authors reported the activation of the inflammatory response through the NF-kB pathway and the consequent release of pro-inflammatory cytokines on lung epithelial cells (Calu-3) infected by SARS-CoV-2. In line with these findings, we found an increase of IL-8 and IL-6 production only on cells primed with PM for 72 h and then exposed to SARS-CoV-2 for additional 24 h. A recent study reported increased production of IL-6 and IL-8 in peripheral blood mononuclear cells (PBMC) from healthy donors treated with PM_{10} and then exposed to SARS-CoV-2, suggesting that the simultaneous exposure to airborne and viral particles could accelerate the inflammatory process (Marín-Palma et al., 2023). Our results confirm that pre-exposure to PM can contribute to the imbalance of the inflammatory response that is typical of COVID-19 patients (Chen et al., 2021; Gudowska-Sawczuk and Mroczko, 2022).

We account for some limitations of our study. The exposure protocol based on submerged conditions is not representative of the actual interaction between the airborne PM/viruses and lung epithelial cells. This could have some effect on the results here reported but, to our understanding, these interferences should be limited (in terms of particles and virus deposition on the cells). Surely, while the concentration of exposure is reported, we could not provide a significant dose of exposure helping to build dose-response functions relevant for toxicological risk assessment. We also acknowledge the limitation of sampling and extracting PM particles from filters. However, for repeated or prolonged exposure conditions, this procedure is still largely valid, enabling to collect enough mass of PM to deliver for toxicological studies.

Furthermore, we are aware that another limitation of this study is related to the cell system selected, based only on a lung epithelial cell type. Several authors reported that biological responses in co-culture of lung epithelial cells with other cell types (endothelial and immune cells) vary substantially with respect to the monoculture (Cappellini et al., 2020; Chary et al., 2019; Loret et al., 2016). The cellular model we used is to be considered a simplification of the complex interaction between different cell types residing in the lungs and may be not completely representative of primary lung cells. Accordingly, our results may underestimate and not cover all the complex feedback that help the

different cell types to maintain lung homeostasis or to amplify the response to biohazard reaching the airways. In the future, the use of complex co-culture systems, also from primary cells, should be better exploited for the understanding of the possible risk factors underlying the appearance and spread of viral infections in relation to a combined or pre-existent exposure to air pollution.

As we report, the SARS-CoV-2 virions we used were inactivated to avoid the biohazard safety requirements needed to use vital viruses. Nonetheless, all the results we provide clearly show that the virions are able to interact with the cell membranes and to enter the cells by endocytosis, while as expected no viral replication was found. Vital viruses, at least to our understanding, may have even an increased adverse toxicological effect, therefore our study may, somehow, underestimate the potency of the combined effect of $PM_{2.5}$ and SARS-CoV-2.

Taken together, these findings provide new insight into the molecular mechanisms through which $PM_{2.5}$ may facilitate the infectivity of a relevant human pathogen (such as SARS-CoV-2) and its effects on lung cells (see Supplementary Fig. 3). Noteworthy, a recent epidemiological population wide (Denmark population cohort - AIRCODEN) study (Zhang et al., 2023) reported that higher incidence and mortality from SARS-CoV-2 infection was significantly associated with exposure to fine PM and NO_2 (as marker of urban vehicles combustion). The data we provide here strongly agree with these epidemiological findings and significantly may help in anticipating or hypothesizing combined effects of air pollutants and other viruses or bacteria.

In fact, we highlight the importance of understanding the role of air pollution in promoting the biological interaction between airborne pathogens (such as bacteria, pollen, fungi, endotoxins, and other viruses) and lung epithelia and the resulting associated pathologies. The times we are living in, in fact, solicit the urgency to carry out a more in-depth investigation, to provide useful elements for understanding the different mechanisms of action of bio-aerosols.

Supplementary data to this article can be found online at https://doi.org/10.1016/j.scitotenv.2024.175979.

CRediT authorship contribution statement

Sara Marchetti: Writing – review & editing, Writing – original draft, Methodology, Investigation, Data curation, Conceptualization. **Anita Colombo:** Writing – review & editing, Investigation. **Melissa Saibene:** Writing – review & editing, Investigation. **Cinzia Bragato:** Writing – review & editing, Investigation. **Teresa La Torretta:** Writing – review & editing, Investigation. **Cristiana Rizzi:** Writing – review & editing, Investigation. **Maurizio Gualtieri:** Writing – review & editing, Supervision, Conceptualization. **Paride Mantecca:** Writing – review & editing, Project administration, Funding acquisition.

Declaration of competing interest

The authors declare that they have no known competing financial interests or personal relationships that could have appeared to influence the work reported in this paper.

Data availability

Data will be made available on request.

Acknowledgement

This work was founded by University of Milano Bicocca, through the Post-doc scholarship to SM. SM, AC, MG, and PM acknowledge the MUSA – Multilayered Urban Sustainability Action – project (ECS 000037), funded by the European Union – NextGenerationEU, under the National Recovery and Resilience Plan (NRRP) Mission 4 Component 2 Investment Line 1.5: Strengthening of research structures and creation of R&D "innovation ecosystems", set up of "territorial leaders in R&D".

References

Abbafati, C., Abbas, K.M., Abbasi, M., Abbasifard, M., Abbasi-Kangevari, M., Abbastabar, H., Lim, S.S., Murray, C.J.L., 2020. Global burden of 369 diseases and injuries in 204 countries and territories, 1990–2019: a systematic analysis for the global burden of disease study 2019. Lancet 396. https://doi.org/10.1016/S0140-6736(20)30925-9.

Atik, N., Wirawan, F., Amalia, R., Khairani, A.F., Pradini, G.W., 2022. Differences in endosomal Rab gene expression between positive and negative COVID-19 patients. BMC. Res. Notes 15. https://doi.org/10.1186/s13104-022-06144-7.

Barhoumi, T., Alghanem, B., Shaibah, H., Mansour, F.A., Alamri, H.S., Akiel, M.A., Alroqi, F., Boudjelal, M., 2021. SARS-CoV-2 coronavirus spike protein-induced apoptosis, inflammatory, and oxidative stress responses in THP-1-like-macrophages: potential role of angiotensin-converting enzyme inhibitor (perindopril). Front. Immunol. 12 https://doi.org/10.3389/fimmu.2021.728896.

Benarroch, Y., Juttukonda, L., Sabharwal, V., Boateng, J., Khan, A.R., Yarrington, C., Wachman, E.M., Taglauer, E., 2021. Differential expression of Rab5 and Rab7 small GTPase proteins in placental tissues from pregnancies affected by maternal coronavirus disease 2019. Clin. Ther. 43, 308–318. https://doi.org/10.1016/j.clinthera.2021.01.002.

Bontempi, E., Vergalli, S., Squazzoni, F., 2020. Understanding COVID-19 diffusion requires an interdisciplinary, multi-dimensional approach. Environ. Res. 188, 109814 https://doi.org/10.1016/j.envres.2020.109814.

Borkotoky, S., Dey, D., Hazarika, Z., 2023. Interactions of angiotensin-converting enzyme-2 (ACE2) and SARS-CoV-2 spike receptor-binding domain (RBD): a structural perspective. Mol. Biol. Rep. 50, 2713–2721. https://doi.org/10.1007/s11033-022-08193-4.

Botto, L., Lonati, E., Russo, S., Cazzaniga, E., Bulbarelli, A., Palestini, P., 2023. Effects of PM2 . 5 Exposure on the ACE / ACE2 Pathway : Possible Implication in COVID-19 Pandemic.

Bozack, A., Pierre, S., DeFelice, N., Colicino, E., Jack, D., Chillrud, S.N., Rundle, A., Astua, A., Quinn, J.W., McGuinn, L., Yang, Q., Johnson, K., Masci, J., Lukban, L., Maru, D., Lee, A.G., 2022. Long-term air pollution exposure and COVID-19 mortality: a patient-level Analysis from new York City. Am. J. Respir. Crit. Care Med. 205 https://doi.org/10.1164/rccm.202104-0845OC.

Cachon, B.F., Firmin, S., Verdin, A., Ayi-Fanou, L., Billet, S., Cazier, F., Martin, P.J., Aissi, F., Courcot, D., Sanni, A., Shirali, P., 2014. Proinflammatory effects and oxidative stress within human bronchial epithelial cells exposed to atmospheric particulate matter (PM2.5and PM>2.5) collected from Cotonou. Benin. Environmental Pollution 185, 340–351. https://doi.org/10.1016/j.envpol.2013.10.026.

Cappellini, F., Di Bucchianico, S., Karri, V., Latvala, S., Malmlöf, M., Kippler, M., Elihn, K., Hedberg, J., Wallinder, I.O., Gerde, P., Karlsson, H.L., 2020. Dry generation of CeO2 nanoparticles and deposition onto a co-culture of A549 and THP-1 cells in air-liquid interface—dosimetry considerations and comparison to submerged exposure. Nanomaterials 10. https://doi.org/10.3390/nano10040618.

Cesar-Silva, D., Pereira-Dutra, F.S., Lucia, A., Giannini, M., Jacques, C., De Almeida, G., 2022. International Journal of Molecular Sciences the Endolysosomal System: The Acid Test for SARS-CoV-2. https://doi.org/10.3390/ijms23094576.

Chary, A., Serchi, T., Moschini, E., Hennen, J., Cambier, S., Ezendam, J., Blömeke, B., Gutleb, A.C., 2019. An in vitro coculture system for the detection of sensitization following aerosol exposure. ALTEX 36, 403–418. https://doi.org/10.14573/altex.1901241.

Chen, H., Liu, W., Wang, Y., Liu, D., Zhao, L., Yu, J., 2021. SARS-CoV-2 activates lung epithelial cell proinflammatory signaling and leads to immune dysregulation in COVID-19 patients. EBioMedicine 70, 103500. https://doi.org/10.1016/j.ebiom.2021.103500.

Chirizzi, D., Conte, M., Feltracco, M., Dinoi, A., Gregoris, E., Barbaro, E., La Bella, G., Ciccarese, G., La Salandra, G., Gambaro, A., Contini, D., 2021. SARS-CoV-2 concentrations and virus-laden aerosol size distributions in outdoor air in north and south of Italy. Environ. Int. 146, 106255 https://doi.org/10.1016/j.envint.2020.106255.

Chu, H., Chan, J.F.-W., Yuen, T.T.-T., Shuai, H., Yuan, S., Wang, Y., Hu, B., Yip, C.C.-Y., Tsang, J.O.-L., Huang, X., Chai, Y., Yang, D., Hou, Y., Chik, K.K.-H., Zhang, X., Fung, A.Y.-F., Tsoi, H.-W., Cai, J.-P., Chan, W.-M., Ip, J.D., Chu, A.W.-H., Zhou, J., Lung, D.C., Kok, K.-H., To, K.K.-W, Tsang, O.T.-Y., Chan, K.-H., Yuen, K.-Y., 2020. Comparative tropism, replication kinetics, and cell damage profiling of SARS-CoV-2 and SARS-CoV with implications for clinical manifestations, transmissibility, and laboratory studies of COVID-19: an observational study. Lancet Microbe 1, e14–e23. https://doi.org/10.1016/s2666-5247(20)30004-5.

Coker, E.S., Cavalli, L., Fabrizi, E., Guastella, G., Lippo, E., Parisi, M.L., Pontarollo, N., Rizzati, M., Varacca, A., Vergalli, S., 2020. The effects of air pollution on COVID-19 related mortality in northern Italy. Environ Resour Econ (Dordr) 76, 611–634. https://doi.org/10.1007/s10640-020-00486-1.

Conticini, E., Frediani, B., Caro, D., 2020. Can atmospheric pollution be considered a co-factor in extremely high level of SARS-CoV-2 lethality in northern Italy? Environ. Pollut. 261, 114465 https://doi.org/10.1016/j.envpol.2020.114465.

Cossart, P., Helenius, A., 2014. Endocytosis of viruses and bacteria. Cold Spring Harb. Perspect. Biol. 6 https://doi.org/10.1101/cshperspect.a016972.

Dergham, M., Lepers, C., Verdin, A., Billet, S., Cazier, F., Courcot, D., Shirali, P., Garçon, G., 2012. Prooxidant and proinflammatory potency of air pollution particulate matter (PM2.5-0.3) produced in rural, urban, or industrial surroundings in human bronchial epithelial cells (BEAS-2B). Chem. Res. Toxicol. 25, 904–919. https://doi.org/10.1021/tx200529v.

Ding, H., Jiang, M., Li, D., Zhao, Y., Yu, D., Zhang, R., Chen, W., Pi, J., Chen, R., Cui, L., Zheng, Y., Piao, J., Schildknecht, S., Gu, N., Kirubakaran Sundar, I., 2021. 12:

662664. Frontiers in Pharmacology | www. Front. Pharmacol 12, 662664. doi:https://doi.org/10.3389/fphar.2021.662664.
Domingo, J.L., Marquès, M., Rovira, J., 2020. Influence of airborne transmission of SARS-CoV-2 on COVID-19 pandemic. A review. Environ Res 188. https://doi.org/10.1016/j.envres.2020.109861.
Fang, Y., Gao, F., Liu, Z., 2019. Angiotensin-converting enzyme 2 attenuates inflammatory response and oxidative stress in hyperoxic lung injury by regulating NF-jB and Nrf2 pathways. Qjm 112, 914–924. https://doi.org/10.1093/qjmed/hcz206.
Garçon, G., Dagher, Z., Zerimech, F., Ledoux, F., Courcot, D., Aboukais, A., Puskaric, E., Shirali, P., 2006. Dunkerque City air pollution particulate matter-induced cytotoxicity, oxidative stress and inflammation in human epithelial lung cells (L132) in culture. Toxicol. In Vitro. https://doi.org/10.1016/j.tiv.2005.09.012.
Giovannoni, F., Li, Z., Remes-Lenicov, F., Dávola, M.E., Elizalde, M., Paletta, A., Ashkar, A.A., Mossman, K.L., Dugour, A.V., Figueroa, J.M., Barquero, A.A., Ceballos, A., Garcia, C.C., Quintana, F.J., 2021. AHR signaling is induced by infection with coronaviruses. https://doi.org/10.1038/s41467-021-25412-x.
Groulx, N., Urch, B., Duchaine, C., Mubareka, S., Scott, J.A., 2018. The pollution particulate concentrator (PoPCon): a platform to investigate the effects of particulate air pollutants on viral infectivity. Sci. Total Environ. 628–629, 1101–1107. https://doi.org/10.1016/j.scitotenv.2018.02.118.
Gualtieri, M., Mantecca, P., Corvaja, V., Longhin, E., Perrone, M.G., Bolzacchini, E., Camatini, M., 2009. Winter fine particulate matter from Milan induces morphological and functional alterations in human pulmonary epithelial cells (A549). Toxicol. Lett. 188, 52–62. https://doi.org/10.1016/j.toxlet.2009.03.003.
Gualtieri, M., Øvrevik, J., Mollerup, S., Asare, N., Longhin, E., Dahlman, H.J., Camatini, M., Holme, J.A., 2011. Airborne urban particles (Milan winter-PM2.5) cause mitotic arrest and cell death: effects on DNA, mitochondria, AhR binding and spindle organization. Mutation Research - Fundamental and Molecular Mechanisms of Mutagenesis 713, 18–31. https://doi.org/10.1016/j.mrfmmm.2011.05.011.
Gudowska-Sawczuk, M., Mroczko, B., 2022. The role of nuclear factor kappa B (NF-κB) in development and treatment of COVID-19: review. Int. J. Mol. Sci. 23 https://doi.org/10.3390/ijms23095283.
Hernandez Carballo, I., Bakola, M., Stuckler, D., 2022. The impact of air pollution on COVID-19 incidence, severity, and mortality: a systematic review of studies in Europe and North America. Environ. Res. 215, 114155 https://doi.org/10.1016/J.ENVRES.2022.114155.
Hoffmann, M., Kleine-Weber, H., Schroeder, S., Krüger, N., Herrler, T., Erichsen, S., Schiergens, T.S., Herrler, G., Wu, N.H., Nitsche, A., Müller, M.A., Drosten, C., Pöhlmann, S., 2020a. SARS-CoV-2 cell entry depends on ACE2 and TMPRSS2 and is blocked by a clinically proven protease inhibitor. Cell 181, 271–280.e8. https://doi.org/10.1016/j.cell.2020.02.052.
Hoffmann, M., Kleine-Weber, H., Schroeder, S., Krüger, N., Herrler, T., Erichsen, S., Schiergens, T.S., Herrler, G., Wu, N.H., Nitsche, A., Müller, M.A., Drosten, C., Pöhlmann, S., 2020b. SARS-CoV-2 cell entry depends on ACE2 and TMPRSS2 and is blocked by a clinically proven protease inhibitor. Cell 181, 271–280.e8. https://doi.org/10.1016/j.cell.2020.02.052.
Hsiao, T.C., Cheng, P.C., Chi, K.H., Wang, H.Y., Pan, S.Y., Kao, C., Lee, Y.L., Kuo, H.P., Chung, K.F., Chuang, H.C., 2022. Interactions of chemical components in ambient PM2.5 with influenza viruses. J. Hazard. Mater. 423, 127243 https://doi.org/10.1016/j.jhazmat.2021.127243.
Hudák, A., Morgan, G., Bacovsky, J., Patai, R., Polgár, T.F., Letoha, A., Pettko-Szandtner, A., Vizler, C., Szilák, L., Letoha, T., 2022. Biodistribution and cellular internalization of inactivated SARS-CoV-2 in wild-type mice. Int. J. Mol. Sci. 23 https://doi.org/10.3390/ijms23147609.
Iwata-Yoshikawa, N., Kakizaki, M., Shiwa-Sudo, N., Okura, T., Tahara, M., Fukushi, S., Maeda, K., Kawase, M., Asanuma, H., Tomita, Y., Takayama, I., Matsuyama, S., Shirato, K., Suzuki, T., Nagata, N., Takeda, M., 2022. Essential role of TMPRSS2 in SARS-CoV-2 infection in murine airways. Nat. Commun. 13 https://doi.org/10.1038/s41467-022-33911-8.
Jalava, P.I., Happo, M.S., Huttunen, K., Sillanpää, M., Hillamo, R., Salonen, R.O., Hirvonen, M.R., 2016. Chemical and microbial components of urban air PM cause seasonal variation of toxicological activity. Environ. Toxicol. Pharmacol. 40, 375–387. https://doi.org/10.1016/j.etap.2015.06.023.
Kelly, F.J., Fussell, J.C., 2012. Size, source and chemical composition as determinants of toxicity attributable to ambient particulate matter. Atmos. Environ. 60, 504–526. https://doi.org/10.1016/j.atmosenv.2012.06.039.
Larsen, B.R., Gilardoni, S., Stenström, K., Niedzialek, J., Jimenez, J., Belis, C.A., 2012. Sources for PM air pollution in the Po plain, Italy: II. Probabilistic uncertainty characterization and sensitivity analysis of secondary and primary sources. Atmos. Environ. 50, 203–213. https://doi.org/10.1016/J.ATMOSENV.2011.12.038.
Li, N., Hao, M., Phalen, R.F., Hinds, W.C., Nel, A.E., 2003. Particulate air pollutants and asthma: a paradigm for the role of oxidative stress in PM-induced adverse health effects. Clin. Immunol. 109, 250–265. https://doi.org/10.1016/J.CLIM.2003.08.006.
Li, S., Zhang, Y., Guan, Z., Li, H., Ye, M., Chen, X., Shen, J., Zhou, Y., Shi, Z.L., Zhou, P., Peng, K., 2020. SARS-CoV-2 triggers inflammatory responses and cell death through caspase-8 activation. Signal Transduct. Target. Ther. 5 https://doi.org/10.1038/s41392-020-00334-0.
Li, H.H., Liu, C.C., Hsu, T.W., Lin, J.H., Hsu, J.W., Li, A.F.Y., Yeh, Y.C., Hung, S.C., Hsu, H.S., 2021. Upregulation of ACE2 and TMPRSS2 by particulate matter and idiopathic pulmonary fibrosis: a potential role in severe COVID-19. Part. Fibre Toxicol. 18 https://doi.org/10.1186/s12989-021-00404-3.
Licen, S., Zupin, L., Martello, L., Torboli, V., Semeraro, S., Gardossi, A.L., Greco, E., Fontana, F., Crovella, S., Ruscio, M., Palmisani, J., Di Gilio, A., Piscitelli, P., Pallavicini, A., Barbieri, P., 2022. SARS-CoV-2 RNA recovery from air sampled on quartz Fiber filters: a matter of sample preservation? Atmosphere (Basel) 13, 1–10. https://doi.org/10.3390/atmos13020340.
Ljunggren, S.A., Nosratabadi, A.R., Graff, P., Karlsson, H., 2019. Monthly variation in masses, metals and endotoxin content as well as pro-inflammatory response of airborne particles collected by TEOM monitors. Air Qual. Atmos. Health 12, 1441–1448. https://doi.org/10.1007/s11869-019-00767-9.
Loaiza-Ceballos, M.C., Marin-Palma, D., Zapata, W., Hernandez, J.C., 2022. Viral respiratory infections and air pollutants. Air Qual. Atmos. Health. https://doi.org/10.1007/s11869-021-01088-6.
Longhin, E., Pezzolato, E., Mantecca, P., Holme, J.A., Franzetti, A., Camatini, M., Gualtieri, M., 2013. Season linked responses to fine and quasi-ultrafine Milan PM in cultured cells. Toxicol. In Vitro 27, 551–559. https://doi.org/10.1016/j.tiv.2012.10.018.
Longhin, E., Camatini, M., Bersaas, A., Mantecca, P., Mollerup, S., 2018. The role of SerpinB2 in human bronchial epithelial cells responses to particulate matter exposure. Arch. Toxicol. 92, 2923–2933. https://doi.org/10.1007/s00204-018-2259-z.
Loret, T., Peyret, E., Dubreuil, M., Aguerre-Chariol, O., Bressot, C., le Bihan, O., Amodeo, T., Trouiller, B., Braun, A., Egles, C., Lacroix, G., 2016. Air-liquid interface exposure to aerosols of poorly soluble nanomaterials induces different biological activation levels compared to exposure to suspensions. Part. Fibre Toxicol. 13 https://doi.org/10.1186/s12989-016-0171-3.
Mantecca, P., Farina, F., Moschini, E., Gallinotti, D., Gualtieri, M., Rohr, A., Sancini, G., Palestini, P., Camatini, M., 2010. Comparative acute lung inflammation induced by atmospheric PM and size-fractionated tire particles. Toxicol. Lett. 198, 244–254. https://doi.org/10.1016/j.toxlet.2010.07.002.
Marchetti, S., Hassan, S.K., Shetaya, W.H., El-Mekawy, A., Mohamed, E.F., Mohammed, A.M.F., El-Abssawy, A.A., Bengalli, R., Colombo, A., Gualtieri, M., Mantecca, P., 2019. Seasonal variation in the biological effects of PM2.5 from greater Cairo. Int. J. Mol. Sci. https://doi.org/10.3390/ijms20204970.
Marchetti, S., Mollerup, S., Gutzkow, K.B., Rizzi, C., Skuland, T., Refsnes, M., Colombo, A., Øvrevik, J., Mantecca, P., Holme, J.A., 2021. Biological effects of combustion-derived particles from different biomass sources on human bronchial epithelial cells. Toxicol. In Vitro 75. https://doi.org/10.1016/j.tiv.2021.105190.
Marchetti, S., Gualtieri, M., Pozzer, A., Lelieveld, J., Saliu, F., Hansell, A.L., Colombo, A., Mantecca, P., 2023. On fine particulate matter and COVID-19 spread and severity: an in vitro toxicological plausible mechanism. Environ. Int. 179, 108131 https://doi.org/10.1016/j.envint.2023.108131.
Marín-Palma, D., Tabares-Guevara, J.H., Zapata-Cardona, M.I., Zapata-Builes, W., Taborda, N., Rugeles, M.T., Hernandez, J.C., Tolbert, W., Jackson, H.M., Cheepsattayakorn, A., Perdomo-Celis, F., 2023. Promotes an Inflammatory Cytokine Response that May Impact SARS-CoV-2 Replication In Vitro OPEN ACCESS EDITED BY, p. PM10. https://doi.org/10.3389/fimmu.2023.1161135.
Miao, L., Yan, C., Chen, Y., Zhou, W., Zhou, X., Qiao, Q., Xu, Z., 2023. SIM imaging resolves endocytosis of SARS-CoV-2 spike RBD in living cells. Cell Chem. Biol. 30, 248–260.e4. https://doi.org/10.1016/j.chembiol.2023.02.001.
Michael, S., Montag, M., Dott, W., 2013. Pro-inflammatory effects and oxidative stress in lung macrophages and epithelial cells induced by ambient particulate matter. Environ. Pollut. https://doi.org/10.1016/j.envpol.2013.01.026.
Michaud, C.M., 2009. Global burden of infectious diseases. Encyclopedia of Microbiology, Third Edition 444–454. https://doi.org/10.1016/B978-012373944-5.00185-1.
Morakinyo, O.M., Mokgobu, M.I., Mukhola, M.S., Hunter, R.P., 2016. Health outcomes of exposure to biological and chemical components of inhalable and respirable particulate matter. Int. J. Environ. Res. Public Health. https://doi.org/10.3390/ijerph13060592.
Murgia, N., Corsico, A.G., Amato, G.D.', Maesano, C.N., Tozzi, A., Annesi-Maesano, I., 2021. Do gene-environment interactions play a role in COVID-19 distribution? The case of Alpha-1 antitrypsin, air pollution and COVID-19 SHORT REPORT ® multidisciplinary respiratory medicine 2021; volume 16:741. Multidiscip. Respir. Med. 16, 5–8.
Nardacci, R., Colavita, F., Castilletti, C., Lapa, D., Matusali, G., Meschi, S., Del Nonno, F., Colombo, D., Capobianchi, M.R., Zumla, A., Ippolito, G., Piacentini, M., Falasca, L., 2021. Evidences for lipid involvement in SARS-CoV-2 cytopathogenesis. Cell Death Dis. 12 https://doi.org/10.1038/s41419-021-03527-9.
Nor, N.S.M., Yip, C.W., Ibrahim, N., Jaafar, M.H., Rashid, Z.Z., Mustafa, N., Hamid, H.H.A., Chandru, K., Latif, M.T., Saw, P.E., Lin, C.Y., Alhasa, K.M., Hashim, J.H., Nadzir, M.S.M., 2021. Particulate matter (PM2.5) as a potential SARS-CoV-2 carrier. Sci. Rep. 11, 1–6. https://doi.org/10.1038/s41598-021-81935-9.
Perrone, M.G., Gualtieri, M., Consonni, V., Ferrero, L., Sangiorgi, G., Longhin, E., Ballabio, D., Bolzacchini, E., Camatini, M., 2013. Particle size, chemical composition, seasons of the year and urban, rural or remote site origins as determinants of biological effects of particulate matter on pulmonary cells. Environ. Pollut. 176, 215–227. https://doi.org/10.1016/j.envpol.2013.01.012.
Pivato, A., Formenton, G., Di Maria, F., Baldovin, T., Amoruso, I., Bonato, T., Mancini, P., Bonanno Ferraro, G., Veneri, C., Iaconelli, M., Bonadonna, L., Vicenza, T., La Rosa, G., Suffredini, E., 2022. SARS-CoV-2 in atmospheric particulate matter: an experimental survey in the province of Venice in northern Italy. Int. J. Environ. Res. Public Health 19, 1–14. https://doi.org/10.3390/ijerph19159462.
Praharaj, M.R., Garg, P., Kesarwani, V., Topno, N.A., Khan, R.I.N., Sharma, S., Panigrahi, M., Mishra, B.P., Mishra, B., Kumar, G.S., Gandham, R.K., Singh, R.K., Majumdar, S., Mohapatra, T., 2022. SARS-CoV-2 spike glycoprotein and ACE2 interaction reveals modulation of viral entry in wild and domestic animals. Front Med (Lausanne) 8, 1–15. https://doi.org/10.3389/fmed.2021.775572.
Romeo, A., Pellegrini, R., Gualtieri, M., Benassi, B., Santoro, M., Iacovelli, F., Stracquadanio, M., Falconi, M., Marino, C., Zanini, G., Arcangeli, C., 2023.

Experimental and in silico evaluations of the possible molecular interaction between airborne particulate matter and SARS-CoV-2. Sci. Total Environ. 895 https://doi.org/10.1016/j.scitotenv.2023.165059.

Saleh, Y., Antherieu, S., Dusautoir, R., Alleman, L.Y., Sotty, J., De Sousa, C., Platel, A., Perdrix, E., Riffault, V., Fronval, I., Nesslany, F., Canivet, L., Garçon, G., Lo-Guidice, J.-M., 2019. Exposure to Atmospheric Ultrafine Particles Induces Severe Lung Inflammatory Response and Tissue Remodeling in Mice. https://doi.org/10.3390/ijerph16071210.

Sancini, G., Farina, F., Battaglia, C., Cifola, I., Mangano, E., Mantecca, P., Camatini, M., Palestini, P., 2014. Health risk assessment for air pollutants: alterations in lung and cardiac gene expression in mice exposed to Milano winter fine particulate matter (PM2.5). PloS One 9. https://doi.org/10.1371/journal.pone.0109685.

Santurtún, A., Colom, M.L., Fdez-Arroyabe, P., Real, Á. del, Fernández-Olmo, I., Zarrabeitia, M.T., 2022. Exposure to particulate matter: direct and indirect role in the COVID-19 pandemic. Environ. Res. 206, 112261. doi:https://doi.org/10.1016/J.ENVRES.2021.112261.

Schreiber, A., Viemann, D., Schöning, J., Schloer, S., Mecate Zambrano, A., Brunotte, L., Faist, A., Schöfbänker, M., Hrincius, E., Hoffmann, H., Hoffmann, M., Pöhlmann, S., Rescher, U., Planz, O., Ludwig, S., 2022. The MEK1/2-inhibitor ATR-002 efficiently blocks SARS-CoV-2 propagation and alleviates pro-inflammatory cytokine/chemokine responses. Cell. Mol. Life Sci. 79, 1–18. https://doi.org/10.1007/s00018-021-04085-1.

Setti, L., Passarini, F., De Gennaro, G., Barbieri, P., Perrone, M.G., Borelli, M., Palmisani, J., Di Gilio, A., Torboli, V., Fontana, F., Clemente, L., Pallavicini, A., Ruscio, M., Piscitelli, P., Miani, A., 2020. SARS-Cov-2RNA found on particulate matter of Bergamo in northern Italy: first evidence. Environ. Res. 188 https://doi.org/10.1016/j.envres.2020.109754.

Shi, J., Du, T., Wang, J., Tang, C., Lei, M., Yu, W., Yang, Y., Ma, Y., Huang, P., Chen, H., Wang, X., Sun, J., Wang, H., Zhang, Y., Luo, F., Huang, Q., Li, B., Lu, S., Hu, Y., Peng, X., 2023. Aryl Hydrocarbon Receptor Is a Proviral Host Factor and a Candidate pan-SARS-CoV-2 Therapeutic Target.

Stracquadanio, M., Petralia, E., Berico, M., La Torretta, T.M.G., Malaguti, A., Mircea, M., Gualtieri, M., Ciancarella, L., 2019. Source apportionment and macro tracer: integration of independent methods for quantification of woody biomass burning contribution to pm10. Aerosol Air Qual. Res. 19, 711–723. https://doi.org/10.4209/aaqr.2018.05.0186.

Valavanidis, A., Fiotakis, K., Vlachogianni, T., 2008. Airborne particulate matter and human health: toxicological assessment and importance of size and composition of particles for oxidative damage and carcinogenic mechanisms. J. Environ. Sci. Health C Environ. Carcinog. Ecotoxicol. Rev. https://doi.org/10.1080/10590500802494538.

Wei, P., Cai, Z., Hua, J., Yu, W., Chen, J., Kang, K., Qiu, C., Ye, L., Hu, J., Ji, K., 2016. Pains and gains from China's experiences with emerging epidemics: from SARS to H7N9. Biomed. Res. Int. 2016 https://doi.org/10.1155/2016/5717108.

Zhang, Y., Sun, H., Pei, R., Mao, B., Zhao, Z., Li, H., Lin, Y., Lu, K., 2021. The SARS-CoV-2 protein ORF3a inhibits fusion of autophagosomes with lysosomes. Cell Discov 7. https://doi.org/10.1038/s41421-021-00268-z.

Zhang, Y.Y., Liang, R., Wang, S.J., Ye, Z.W., Wang, T.Y., Chen, M., Liu, J., Na, L., Yang, Y. L., Yang, Y.B., Yuan, S., Yin, X., Cai, X.H., Tang, Y.D., 2022. SARS-CoV-2 hijacks macropinocytosis to facilitate its entry and promote viral spike–mediated cell-to-cell fusion. J. Biol. Chem. 298, 102511 https://doi.org/10.1016/j.jbc.2022.102511.

Zhang, J., Lim, Y.H., So, R., Jørgensen, J.T., Mortensen, L.H., Napolitano, G.M., Cole-Hunter, T., Loft, S., Bhatt, S., Hoek, G., Brunekreef, B., Westendorp, R., Ketzel, M., Brandt, J., Lange, T., Kølsen-Fisher, T., Andersen, Z.J., 2023. Long-term exposure to air pollution and risk of SARS-CoV-2 infection and COVID-19 hospitalisation or death: Danish nationwide cohort study. Eur. Respir. J. 62 https://doi.org/10.1183/13993003.00280-2023.